Research article

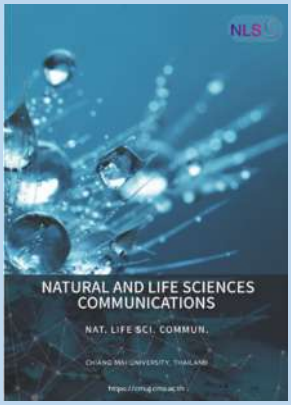

Editor:
Laongnuan Srisombat,
Chiang Mai University, Thailand

Article history:
Received: April 17, 2023;
Revised: July 1, 2023;
Accepted: July 10, 2023;
Online Frist: August 9, 2023;
https://doi.org/10.12982/NLSC.2023.057

Corresponding author:
Sirivan Athikomkulchai
E-mail: sirivan@g.swu.ac.th

Cytotoxicity, Apoptosis Induction, Oxidative Stress, and Cell Cycle Arrest of *Clerodendrum chinense* Flower Extract Nanoparticles in HeLa Cells

Chuda Chittasupho[1], Weerasak Samee[2], Sarin Tadtong[3], Wullapa Jittachai[3], Chittima Managit[4], and Sirivan Athikomkulchai[3, *]

1 Department of Pharmaceutical Sciences, Faculty of Pharmacy, Chiang Mai University, Mueang, Chiang Mai 50200 Thailand.
2 Department of Pharmaceutical Chemistry, Faculty of Pharmacy, Srinakharinwirot University, Ongkharak, Nakhon Nayok 26120 Thailand.
3 Department of Pharmacognosy, Faculty of Pharmacy, Srinakharinwirot University, Ongkharak, Nakhon Nayok 26120 Thailand.
4 Department of Pharmaceutical Technology, Faculty of Pharmacy, Srinakharinwirot University, Ongkharak, Nakhon Nayok 26120 Thailand.

ABSTRACT

Clerodendrum chinense is a plant containing numerous secondary active metabolites. This study aimed to evaluate the antioxidant and anti-cancer activities of *C. chinense* flower ethanolic extract and identify the bioactive compounds. High-performance liquid chromatography was used to identify and quantify the bioactive compounds of the extract. The antioxidant activity of the extract was determined using the 2,2-diphenyl-1-picrylhydrazyl (DPPH) and 2,2'-azino-bis(3-ethylbenzothiazoline-6-sulfonic acid (ABTS) free radical scavenging assays and the Ferric Reducing Antioxidant Power Assay (FRAP). The cytotoxicity of *C. chinense* flower ethanolic extract against A549, MCF-7 and HeLa cells was determined using the sulforhodamine B (SRB) assay. Nanoparticles (NPs) of *C. chinense* flower extract were fabricated using a solvent displacement method. Then the anti-cancer activities of the extract and NPs were confirmed by cytotoxicity, cell apoptotic induction, reactive oxygen species (ROS) formation, colony formation and cell cycle assays against HeLa cervical cancer cells. *C. chinense* flower extract and NPs showed significant free radical scavenging activities and ferric-reducing power. As shown by Pearson's correlation coefficients, the total phenolic and total flavonoid contents of *C. chinense* flower extract and NPs significantly correlated with antioxidant activity. *C. chinense* flower extract demonstrated antiproliferative activity against A549, MCF-7 and HeLa cancer cells after treatment for 24, 48 and 72 h. The growth inhibition of HeLa cells mediated by *C. chinense* flower extract and NPs appears to be associated with apoptosis, ROS formation and cell cycle arrest. Thus, this study provided evidence of the anticervical cancer potentials of *C. chinense* flower ethanolic extract and NPs.

Keywords: Natural products, Nanoparticles, Pharmaceutical, Phenolic compounds, Plant extract, *Clerodendrum chinense*

Funding: This work was supported by the Faculty of Pharmacy, Srinakharinwirot University (Grant No. 236/2565) and partially supported by Chiang Mai University.

Citation: Chittasupho, C., Samee, W., Tadtong, S., Jittachai, W., Managit, C., and Athikomkulchai, S. 2023. Cytotoxicity, apoptosis induction, oxidative stress, and cell cycle arrest of *Clerodendrum chinense* flower extract nanoparticles in HeLa cells. Natural and Life Sciences Communications. 22(4): e2023057.

INTRODUCTION

Reactive oxygen species (ROS) levels are elevated in almost all cancers, promoting many aspects of tumor development and progression. Antioxidant agents may be able to interfere with carcinogenesis since oxidative stress has been linked to cancer onset and progression by increasing DNA mutations or inducing DNA damage, genome instability and cell proliferation (Reuter et al., 2010). Conventional radio-/chemotherapies are well known to influence tumor outcomes via ROS modulation (Mileo et al., 2016). Many natural polyphenols have emerged as promising bioactive anticancer compounds. Polyphenols have been discovered to have a dominant antioxidant that reduces oxidative stress caused by pathologic conditions such as cancer. They play an important role in regulating the mammalian epigenome *via* mechanisms and proteins that remodel chromatin (Rajendran P. et al., 2022). Polyphenols can influence epigenetic modifications such as DNA methylation, histone modifications and noncoding miRNA expression, influencing gene expression. These epigenetic changes, producing polyphenols and other phytochemicals, are critical in treating and preventing cancer prevention. Polyphenol scavenges reactive oxygen species (ROS) and reduces oxidative damage to biomolecules (Zhang Hua et al., 2016). Polyphenols with antioxidant capacity inhibit the signaling pathways involved in generating oxidative stress at the molecular level.

Clerodendrum chinense is a flowering plant in the genus *Clerodendrum*, family Lamiaceae. Abourzid et al. reported that *Clerodendrum chinense* and *Clerodendrum splendens* flower chloroform extracts effectively inhibited the growth of *Plasmodium falciparum* with an IC_{50} value of less than 10 µg/mL. Chloroform extracts of *C. chinense* stem and flowers can inhibit *Trypanosoma cruzi* with marginal cytotoxicity with IC_{50} values of 1.21 and 1.12 µg/mL, respectively (Abouzid et al., 2013). The anti-cancer activities of leaves and root of *C. chinense* extracts have been previously reported. We have recently showed that *C. chinense* leaf extract had cytotoxicity against A549 lung cancer cells in a dose-dependent manner with the IC_{50} of 340.6 µg/mL after treating with the cells for 24 h. The extract also inhibited formation of lung cancer cell colony and cell migration (Chittasupho et al., 2023a). Barung et al described the anti-cancer activities of *C. chinense* leaf fractions obtained from ethanol, hexane, ethyl acetate, and water solvent extraction with the IC_{50} values of 436.9, 295.7, 191,2, and 373.8 µg/mL, respectively (Barung et al., 2021). In addition, the study by Chen et al. suggested that *C. chinense* root extract can reduce the number of promyelocytic cell line (HL-60) in a time-dependent manner and blocked the differentiation of HL-60 cells into mature monocytoid cells (Chen et al., 1988). Qi et al demonstrated that the isolated diterpenoids from *C. chinense* extract displayed strong antiproliferative activities against A549 lung cancer cells and HL-60 human leukemia cell line (Qi et al., 2021).

Nanoparticles have drawn the attention of researchers due to the enhanced permeability and retention effects (EPR), leading to the accumulation of active drugs in tumor tissues. This process, known as passive targeting, is based on the small size of nanoparticles and the leaky vasculature and impaired lymphatic drainage of neoplastic tissues. The other benefits of nanoparticles are their targetability, increasing the water solubility of encapsulated drugs, enhancing permeability and retention effect, biocompatibility, reducing toxicity, high stability, high loading capacity, the feasibility of incorporating both hydrophilic and hydrophobic substances and feasibility of variable routes of administration (Gavas et al., 2021). The various therapeutic implications of nanoformulations have opened new avenues for cancer treatment.

Fabrication of nanoparticles (NPs) to deliver plant crude extract has shown several advantages. *Clerodendrum quadrangulare* Kurz leaf extract NPs improved the colloidal stability of the extract and showed cell growth inhibition

activity, apoptosis-inducing activity and cell cycle arrest (Chittasupho et al., 2018). In another study, NPs of *Pluchea indica* L. (Less) leaf extract demonstrated increased migration of oral mucosal cells at low concentrations. The NPs increased colloidal stability compared with the crude extract in an oral spray formulation (Buranasukhon et al., 2017). Nanoparticles of *P. indica* branch extracts improved colloidal stability and cell migration in an *in vitro* wound healing assay (Chiangnoon et al., 2022).

The present study aimed to evaluate the antioxidant and cytotoxicity of *C. chinense* flower extract. *C. chinense* flower extract's nanoparticles were formulated, characterized and investigated for their antioxidant and anticancer activities and compared with the crude extract. The study covers the effects of *C. chinense* flower extract on HeLa cells, A549 cells, and MCF-7 cells. The effects of extract and NPs on cancer cell viability, apoptosis, ROS formation, colony formation and cell cycle arrest were further investigated on the cell line that was mostly sensitive to the extract in the first 24 h. Our results suggested that *C. chinense* flower extract and NPs may be exploited to develop potentially promising functional nanomaterials for DNA-damage-induced treatment in cancer therapy. However, the possible mechanisms of their effects on HeLa cells needs further investigation.

MATERIALS AND METHODS

Materials

Quercetin (98% purity) and epigallocatechin (EGCG) (98% purity) were purchased from Chanjao Longevity Co., Ltd., Bangkok, Thailand. Acetonitrile (HPLC grade) 95% ethanol and 1 N sodium hydroxide were purchased from Qrec (Kuala Lumpur, Malaysia). Folin–Ciocalteau phenol reagent, aluminum chloride, ferric chloride and gallic acid were obtained from Loba Chemie, Mumbai, India. A549 (CCL-185™), MCF-7 (HTB-22™) and HeLa (CCL-2™) cells were purchased from the American Type Culture Collections (Manassas, VA, USA). Dulbecco's Modified Eagle Medium (DMEM), fetal bovine serum, 100 U/mL penicillin and 100 µg/mL streptomycin and Trypsin-EDTA were purchased from Invitrogen, Carlsbad, CA, USA). DPPH (2,2-diphenyl-1-picrylhydrazyl), ABTS (2,2’-azino-bis(3-ethylbenzothiazoline-6-sulfonic acid)), sulforhodamine B (SRB), and acridine orange/ethidium bromide (AO/EB) and DCF-DA were purchased from Sigma Merck KGaA (Darmstadt, Germany).

Plant collection and identification

C. chinense flowers were collected from plants grown at the GPS coordinates 14°06’27.4’’N 100°59’06.1’’E *C. chinense* was identified by Sirivan Athikomkulchai. A voucher specimen (SIRA003) was deposited at the herbarium of Srinakharinwirot University, Nakhon Nayok, Thailand.

C. chinense flower extraction

C. chinense flowers were dried at 50°C for 48 h in a hot air oven and ground to powder. The powdered plant material (5 g) was extracted with 95% ethanol (50 mL) by maceration for 72 h. The plant powder was repeatedly macerated two more times. The crude extract was filtered through cloth three times. After filtering the extracts, the extraction solvent was evaporated under reduced pressure with a rotary vacuum evaporator until the concentrated crude extract was obtained. The yield (%w/w) of the extract was calculated using the following equation.

$$Yield\ (\%) = \frac{Weight\ of\ extract}{Weight\ of\ dried\ powder} \times 100\% \quad (1)$$

Preparation and characterization of nanoparticles containing *C. chinense* flower ethanolic extract

Nanoparticles of *C. chinense* flower ethanolic extract were fabricated using a solvent displacement method (Chittasupho et al., 2010). *C. chinense* flower ethanolic extract (200 mg) was dissolved in 2 mL of 95% ethanol and infused in 15 mL of 0.1% w/v poloxamer 407 at a rate of 1 mL/h under magnetic stirring (700 rpm). To remove the organic solvent, the NP mixture was stirred overnight under the fume hood at room temperature. A dynamic light scattering (DLS) method was used to assess the size, polydispersity index value (PDI) and zeta potential of *C. chinense* flower extract NPs (1.3 mg/mL) at a 173° scattering angle and 25°C (Zetasizer Nanoseries, Malvern instruments, Malvern, UK).

The morphology of *C. chinense* flower extract nanoparticles was observed using a transmission electron microscope (TEM) (FEI Tecnai G2 20 200kV TEM/STEM/EDX/Tomography, OR, USA). A drop of nanoparticle suspension was deposited on a copper grid with carbon film and dried at room temperature. After another drop was repeatedly deposited on the grid, samples were allowed to dry at room temperature before investigation.

Determination of physical stability of *C. chinense* flower ethanolic extract nanoparticles

The physical stability including temperature and time stabilities of *C. chinense* flower ethanolic extract nanoparticles was investigated in terms of temperature and time. *C. chinense* flower ethanolic extract nanoparticles (13.33 mg/mL) in deionized water were placed in a tight container and stored at 4°C, 30°C, and 45°C for 6 months. A dynamic light scattering technique (Zetasizer ZS, Malvern, UK) was used to determine the hydrodynamic diameter, polydispersity value and zeta potential value of the NPs at certain time intervals (0, 1, 2, 4 and 6 months) to monitor the effect of storage conditions on the size, polydispersity and surface charge of the NPs.

Determination of total phenolics in *C. chinense* flower extract and nanoparticles

Folin-Ciocalteu reagents were used to determine total phenolics. *C. chinense* flower extract at the concentrations ranging from 39 to 20,000 µg/mL. *C. chinense* flower extract NPs at the concentrations ranging from 26 to 13,333 µg/mL and gallic acid standard solution at the concentrations ranging from 3.9 to 2000 µg /mL (50 µL/well) were mixed with 10% v/v Folin-Ciocalteu reagent (100 µL) and allowed to stand at room temperature for 5 min before adding 7.5%, w/v sodium bicarbonate (50 µL). After 2 h incubating at room temperature, absorbance at 765 nm was measured (Spectramax M3, Thermo Scientific, Waltham, MA, USA). Gallic acid absorbance was plotted against concentration and used to create a calibration curve. The results were expressed in milligrams of gallic acid equivalents (GAE) per gram of dry extract. The chemical stability of *C. chinense* flower extract NPs stored at 4°C for 2 months was investigated using a quantitative analysis of total phenolic content in the nanoparticles.

Determining total flavonoids in *C. chinense* flower extract and nanoparticles

The total flavonoid levels in *C. chinense* flower extract were determined using the aluminum chloride colorimetric method. In 96-well plates, quercetin and epigallocatechin gallate (EGCG) solutions (3.9-2000 µg/mL), *C. chinense* flower extract (39-20,000 g/mL) and *C. chinense* flower extract NPs (26-13,333 µg/mL) (100 µL/well) were added. Each well was filled with sodium nitrate (5% w/v, 30 µL) and incubated for 5 min. The mixture was then incubated for 6 min with a 2% w/v aluminum chloride solution before being incubated for another 10 min with 1 N sodium hydroxide. A UV-Vis spectrophotometer and a microplate reader were used to measure the absorbance at 510 nm (Spectramax M3, Thermo Scientific, Waltham, MA, USA). The data were presented as mg quercetin equivalents (QE) and EGCG equivalents per g of dry extract using the quercetin and EGCG standard curves. The chemical stability of *C. chinense* flower extract NPs stored at 4°C for 2 months was investigated by a quantitative analysis of total flavonoid content in the nanoparticles.

Identification and quantification of bioactive compounds in *C. chinense* flower extract using high-performance liquid chromatography (HPLC)

The bioactive compounds, verbascoside, isoverbascoside and hispidulin, were identified and quantified in the *C. chinense* flower extract using an HPLC (YL9100 Plus HPLC) on RP- C18 column (ACE 5 C18-AR, 250 × 4.6 mm, 5 µm). The mobile phase consisted of acetonitrile (A) and 0.085% phosphoric acid in water (B) in a gradient elution mode. The gradient elution initial conditions were 5% of eluent A with a linear gradient to 40% from 0.01 to 20 min, followed by a linear gradient to 80% of eluent A at 30 min, and this proportion was maintained for 5 min. The mobile phase composition returned to the initial condition at 5 min and was allowed to run for another 10 min before the injection of another sample, and the flow rate was set at 1.0 ml/min. The injection volume was 50 µL. A vacuum was used for degassing the solvents. A 0.45 µm membrane filter was used to filter samples before HPLC analysis, and a UV-visible detector (YL9120 UV/VIS) was used to monitor the peaks at 326 nm. The peaks were identified based on retention time, and their contents in the extracts were quantified using calibration curves plotted between peak area and standard concentration.

Antioxidant assay

Determination of DPPH free radical scavenging activity of *C. chinense* flower extract and NPs

The free radical scavenging activity of *C. chinense* flower extract and NPs was determined using the DPPH assay. Extract concentrations ranging from 39 to 20,000 µg/mL were diluted in 95% ethanol. NPs of *C. chinense* flower extract were diluted in deionized water at concentrations ranging from 26 to 13,333 µg/mL. A clear quercetin solution at concentrations ranging from 3.9 to 2,000 µg/mL was used as a positive control. In absolute ethanol, a 100 µL solution of quercetin, *C. chinense* flower extract and NPs were mixed with a 100 µL of 500 µM DPPH. The mixture was incubated at room temperature in the dark for 30 min. After incubating, the absorbance was measured with a UV-Vis spectrophotometer microplate reader at 517 nm (Warinthip; et al., 2023). Equation (2) was used to calculate the percentage of radical scavenging activity. The concentration of samples that scavenge 50% of the DPPH free radical (IC_{50}) was calculated by GraphPad Prism, Version 7.0.

$$\text{DPPH free radical scavenging } (\%) = \frac{(A-B)}{A} \times 100\% \qquad (2)$$

where A is the absorbance of the reaction with solvent control and B is the absorbance of reaction with the samples. The DPPH free radical scavenging activity of the NPs was investigated after storing at 4°C for 2 months.

Determination of ABTS free radical scavenging activity of *C. chinense* flower extract and NPs

Quercetin was diluted in deionized water ranging from 3.9 to 2,000 µg/mL. The flower extract and NPs of *C. chinense* were diluted in 95% ethanol or deionized water at concentrations ranging from 39 to 20,000 µg/mL and 26 to 13,333 µg/mL, respectively. ABTS radical cation (ABTS+·) was produced by reacting to an ABTS ethanolic stock solution (7 mM) with a 2.45 mM potassium persulfate solution in the dark for 24 h before use. After diluting the ABTS+· radical solution with absolute ethanol, the absorbance at 734 nm was 0.70 ± 0.02. Quercetin, *C. chinense* flower extract and NPs (180 µL) were incubated for 15 min at room temperature in the dark with an ABTS+· solution (20 µL). Absorbance was determined using a UV-Vis spectrophotometer. The percentage of ABTS+·radical scavenging activity was calculated using Equation (3). The concentration of samples that scavenge 50% of the ABTS free radical (IC_{50}) was calculated by GraphPad Prism, Version 7.0.

$$\text{ABTS free radical scavenging } (\%) = \frac{(A-B)}{A} \times 100\% \qquad (3)$$

where A is the absorbance of the reaction with solvent control and B is the absorbance of the reaction with the samples.

Determination of ferric reducing antioxidant power (FRAP) of *C. chinense* flower extract and NPs

The antioxidant power of *C. chinense* flower extract and NPs to reduce ferric was measured and compared with quercetin. The FRAP reagent comprised 10 mM TPTZ in 40 mM HCl, 20 mM $FeCl_3 6H_2O$ and 300 mM (pH 3.6) acetate buffer. A total of 180 µL of FRAP reagent was thoroughly mixed with 20 µL of *C. chinense* flower extract (39-20,000 µg/mL), NPs (26-13,333 µg/mL) or quercetin (3.9 to 2,000 µg/mL). The absorbance at 595 nm was measured after incubating 30 min at 37°C. The standard curve was created with a ferrous sulfate solution (9.8-2,500 µM), and the results were expressed in µmol Fe (II) equivalents.

Determination of cytotoxicity and antiproliferation of *C. chinense* flower extract using sulforhodamine B (SRB) assay

Cell culture

HeLa, A459 and MCF-7 cancer cells were cultured in DMEM complete medium with 10% fetal bovine serum, 100 U/mL penicillin G and 100 µg/mL streptomycin at 37°C and 5% CO_2. The DMEM medium was replaced every three days, trypsinized with 0.25% trypsin-EDTA and subcultured in the same medium.

Cell viability assay

Sulforhodamine B (SRB) assay is a colorimetric assay to evaluate cell death by binding SRB to cell proteins. HeLa, A459 and MCF-7 cells were placed (1×10^4 cells/well) in a 96-well plate and incubated for 24 h. The cells were

treated for 24 h with different concentrations of *C. chinense* flower extract (0, 25, 50, 100, 250, 500 and 1,000 µg/mL) and then removed. Cell viability was examined 24 h, 48 h and 72 h after exposure to the extract. The cells were fixed with ice-cold 10% w/v trichloroacetic acid at 4°C and stained for 30 min at room temperature with 0.4% SRB dye. Excess dye was removed by repeated washing with 1% acetic acid. The dye bound to the cells was solubilized by 10 mm mM Tris base buffer (200 µL, pH 8.0), and the absorbance was measured at 540 nm with a spectrophotometer microplate reader (Spectramax M3, Molecular Devices, Invitrogen, USA). The % cell viability was calculated using the following equation: control was untreated cells.

$$Cell\ viability\ (\%) = \frac{A540\ sample}{A540\ control} \times 100 \quad (4.)$$

The IC_{50} values for *C. chinense* flower extract and nanoparticles were determined by using GraphPad Prism software. Prism built equations where X values are logarithms of concentration and Y values are %cell viability. The dose-response curve of %cell viability and log concentration followed a sigmoidal shape. The IC_{50} value of %cell viability refers to a concentration of *C. chinense* flower extract and nanoparticles required to bring the curve down to a point halfway between the maximal to the minimal plateaus of the curve, which was calculated by GraphPad Prism 7.

Apoptosis assay using acridine orange/ethidium bromide (AO/EB) staining method

The AO/EB fluorescent dye was used to detect apoptosis-associated changes in cell membranes during the apoptosis of cancer cells. For 24 h, HeLa cancer cells (1×10^4 cells/well) were seeded in a 96-well culture plate and exposed to different doses of *C. chinense* flower extract (100, 250 and 500 µg/mL) and NPs (250, 500 and 1,000 µg/mL). The HeLa cells were incubated in a dye mixture containing AO (1 µg/mL) and EB (1 µg/mL) in a 1:1 ratio for 15 min at room temperature in the dark. The culture plate was immediately visualized under a fluorescence microscope (20x magnification, Nikon Eclipse TS100 inverted microscope, Tokyo, Japan), and images were taken.

ROS formation assay

In 6-well plates, HeLa cells were seeded at $2x10^5$ cells/well density and incubated for 24 h with *C. chinense* flower extract (100, 250 and 500 µg/mL) and NPs (250, 500 and 1,000 µg/mL). The cell was then trypsinized and incubated for 30 min at 37°C in the dark in a new complete DMEM culture medium containing 25 µM 2′,7′-dichlorofluorescin diacetate (DCF-DA). ROS generation was determined using BD Accuri™ flow cytometry (BD Biosciences, San Jose, CA, USA) and fluorescent signals were displayed as histograms (.BD Accuri C6 Plus software).

Colony formation assay

The colony-forming or clonogenic assay is a quantitative *in vitro* technique to assess a single cell's ability to proliferate in a large colony via clonal expansion. HeLa cells were cultured for 24 h with *C. chinense* flower extract (0, 25, 50, 100, 250, 500 and 1,000 µg/mL) or NPs (0, 50, 100, 250, 500 and 1,000 µg/mL) before being shifted to DMEM medium and cultured for another 15 days. The cells were stained with 0.5% crystal violet, washed with deionized water, air-dried and photographed. A colony was defined as

containing at least 50 cells. The number of cells counted was compared with that of a control group.

Cell cycle analysis

Flow cytometry was used to examine the effect of the extract on the cell cycle distribution of HeLa cancer cells. Briefly, 2.5×10^5 cells/mL were plated onto a 6-well cultured plate for 24 h before different doses of *C. chinense* flower extracts (100, 250 and 500 µg/mL) and NPs (250, 500 and 1,000 µg/mL) were added to each well for a 24-hour incubation period. Cells were trypsinized, washed with PBS buffer, and fixed in -20°C ice-cold 70% ethanol. Then the cancer cells were exposed to PI solution (BD Biosciences, CA, USA) for 30 min at 4°C. The cell cycle phases were analyzed using a flow cytometer (BD Biosciences, CA, USA) and fluorescent signals were displayed as histograms. Cell cycle stages were gated manually.

Statistical analysis

The data were statistically evaluated using an analysis of variance (one-way ANOVA). The Newman-Keuls test was used as a post hoc test to determine significant differences. The t-test was used to compare the significance of the differences between the mean of the two groups; in all cases, P <0.05 was considered significant.

RESULTS

Yield of *C. chinense* flower ethanolic extract

C. chinense flower extract was concentrated and dried under reduced pressure using a rotary evaporator after maceration with 95% ethanol. After weighing the dried extract, the yield was calculated to be 11.40% w/w.

Characterization of *C. chinense* flower ethanolic extract and NPs

The average hydrodynamic diameter, polydispersity index (PDI) and zeta-potential value of freshly prepared *C. chinense* flower ethanolic extract NPs were 135.43 ± 23.14 nm, 0.31 ± 0.07 and −20.50 ± 2.48 mV, respectively. The mean particle size, PDI and zeta potential values of *C. chinense* flower ethanolic extract NPs after storing for 1, 2, 4 and 6 months are presented in Figure 1A. The sizes of the NPs after fresh preparation and storing for 6 months ranged from 104.67 ± 2.89 to 225.97 ± 10.09 nm. The PDI of the NPs after fresh preparation and after storing for 6 months ranged from 0.21 ± 0.01 to 0.40 ± 0.02 (Figure 1B). The zeta potential values of the NPs after fresh preparation and storing for 6 months ranged from -7.18 ± 0.74 to -21.90 ± 0.79 mV (Figure 1C). The size of the NPs stored for 6 months were well maintained, confirming the excellent stability of this NPs (Song et al., 2021). The size of the NPs was confirmed by transmission electron microscope image as shown in Figure 1D.

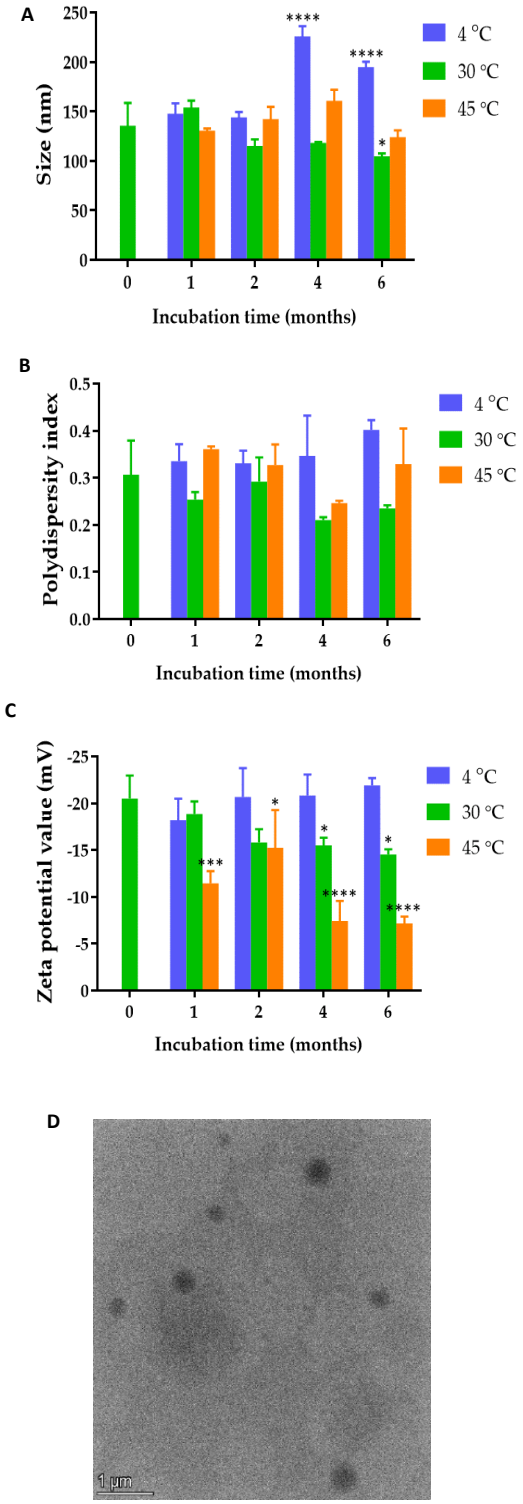

Figure 1. (A) Hydrodynamic diameter (B) polydispersity index and (C) zeta potential values of *C. chinense* flower extract NPs after fresh preparation and storing in deionized water for 1, 2, 4 and 6 months at 4, 30 and 45°C. (D) Transmission electron microscope image of *C. chinense* flower extract. The data represent mean ± SD of three experiments. *, ***, and **** indicate P <0.05, P <0.001 and P <0.0001 compared with day 0, respectively.

Total phenolic and flavonoid contents of *C. chinense* flower extract and NPs

The total phenolic contents in *C. chinense* flower extract was determined by the Folin-Ciocalteu method using the gallic acid standard curve. The total phenolic contents of *C. chinense* ethanolic flower extract and NPs increased with the concentration of the extract and NPs (Figure 2A). The average total phenolic contents in *C. chinense* flower extract and the NPs were 487.44 ± 32.43 and 449.73 ± 22.68 mg GAE per g of dry extract, respectively. The total content of flavonoids in *C. chineses* flower extract was quantified using the aluminum chloride colorimetric assay. The aluminum chloride colorimetry results showed that the total flavonoid contents of *C. chinense* ethanolic flower extract and NPs increased with the concentration (Figure 2B). The total flavonoid content in *C. Chinese* flower extract and NPs were averaged at 199.86 ± 61.03 and 161.84 ± 22.47 mg QE per g of dry extract, respectively. The chemical stability results showed that total phenolic content in *C. chinense* flower extract NPs reduced to 88.96 ± 0.94% and 85.36 ± 1.35% after storing at 4°C for 1 and 2 months, respectively. The total flavonoid content was decreased to 94.16 ± 19.48% and 93.49 ± 3.64%, after storing 1 and 2 months, respectively.

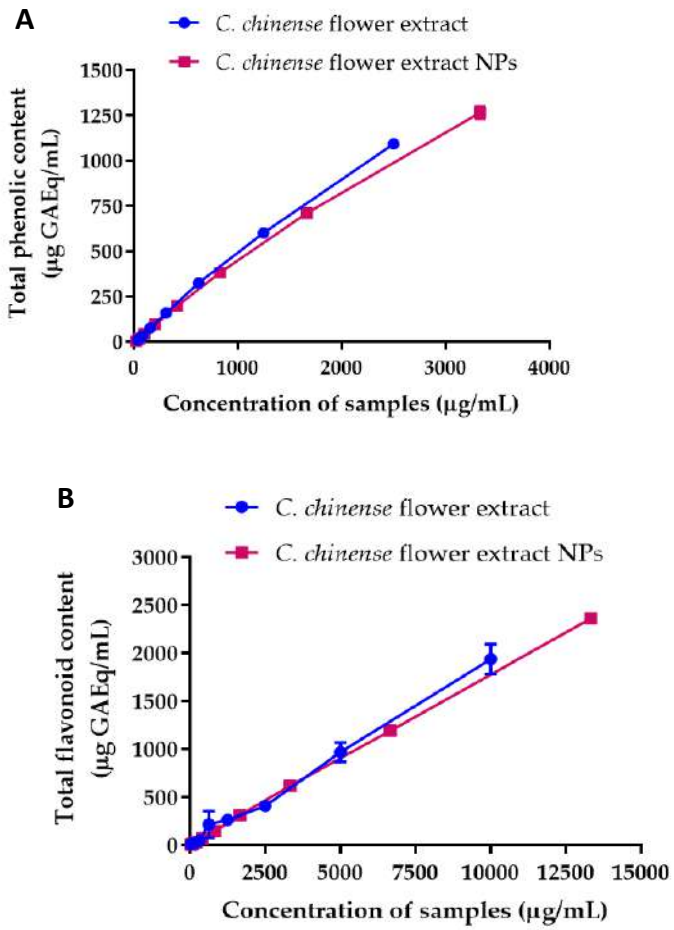

Figure 2. (A) Total phenolic content of *C. chinense* flower extract and NPs, (B) total flavonoid content of *C. chinense* flower extract and NPs.

Bioactive compounds in *C. chinense* flower extract determined by HPLC analysis

The phenolic compounds and flavonoids in *C. chinense* flower extracts were identified and quantified using reversed-phase HPLC. The HPLC analysis result indicated that *C. chinense* flower extract contained verbascoside, isoverbascoside and hispidulin as major compounds. The chromatograms suggested that verbascoside, isoverbascoside and hispidulin were found in the extract (Figure 3). The retention times of verbascoside, isoverbascoside, and hispidulin standards were 16.6, 17.4 and 25.7 min, respectively. *C. chinense* chromatogram showed peaks at retention times of 16.6, 17.4 and 25.7 min. These results indicated that *C. chinense* flower extract contained verbascoside, isoverbascoside and hispidulin. Verbascoside was the major phytochemical compound in *C. chinense* ethanolic extract with an amount of 11.27 ± 0.08 µg/mg extract. Isoverbascoside was present at 4.30 ± 0.27 µg/mg extract, and hispidulin was contained at 0.98 ± 0.01 µg/mg extract. The standard curves of verbascoside, isoverbascoside, and hispidulin are shown in Figure 4.

The presence of verbascoside, isoverbascoside and hispidulin in *C. chinense* flower ethanolic extract has been reported before. However, verbascoside, isoverbascoside decaffeoylverbascoside, hispidulin, lupeol and icariside B5 were isolated from the leaves of *C. chinense*. Verbascoside showed significant analgesic, antiinflammatory and antipyretic effects (Abouzid et al., 2013; Wahba et al., 2011).

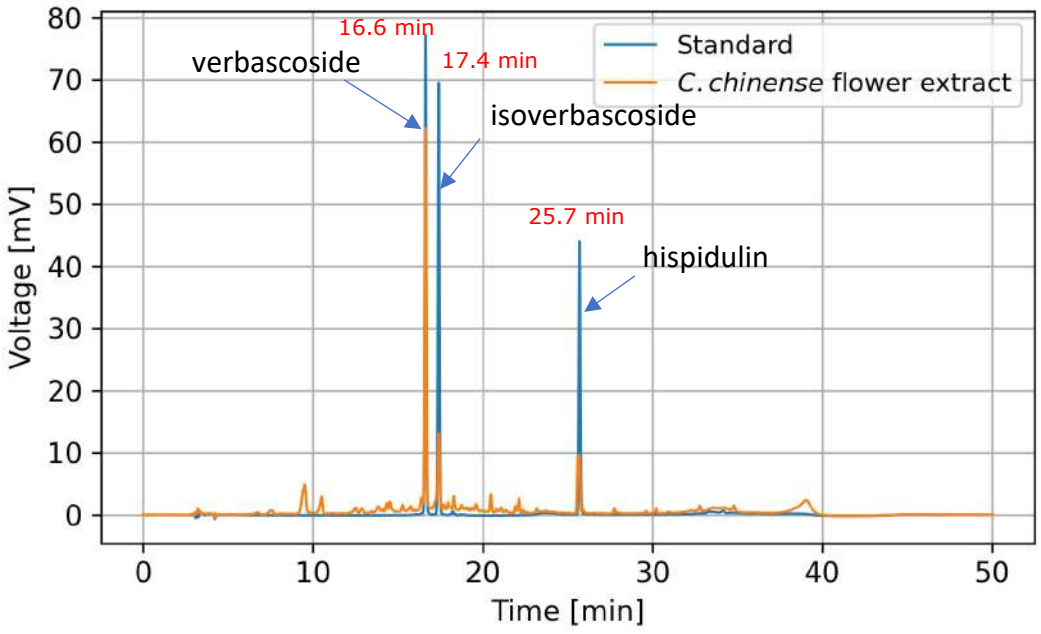

Figure 3. Overlayed HPLC chromatogram of verbascoside (5 µg/mL), isoverbascoside (5 µg/mL), hispidulin (0.9 µg/mL) standards and *C. chinense* flower extract (200 µg/mL).

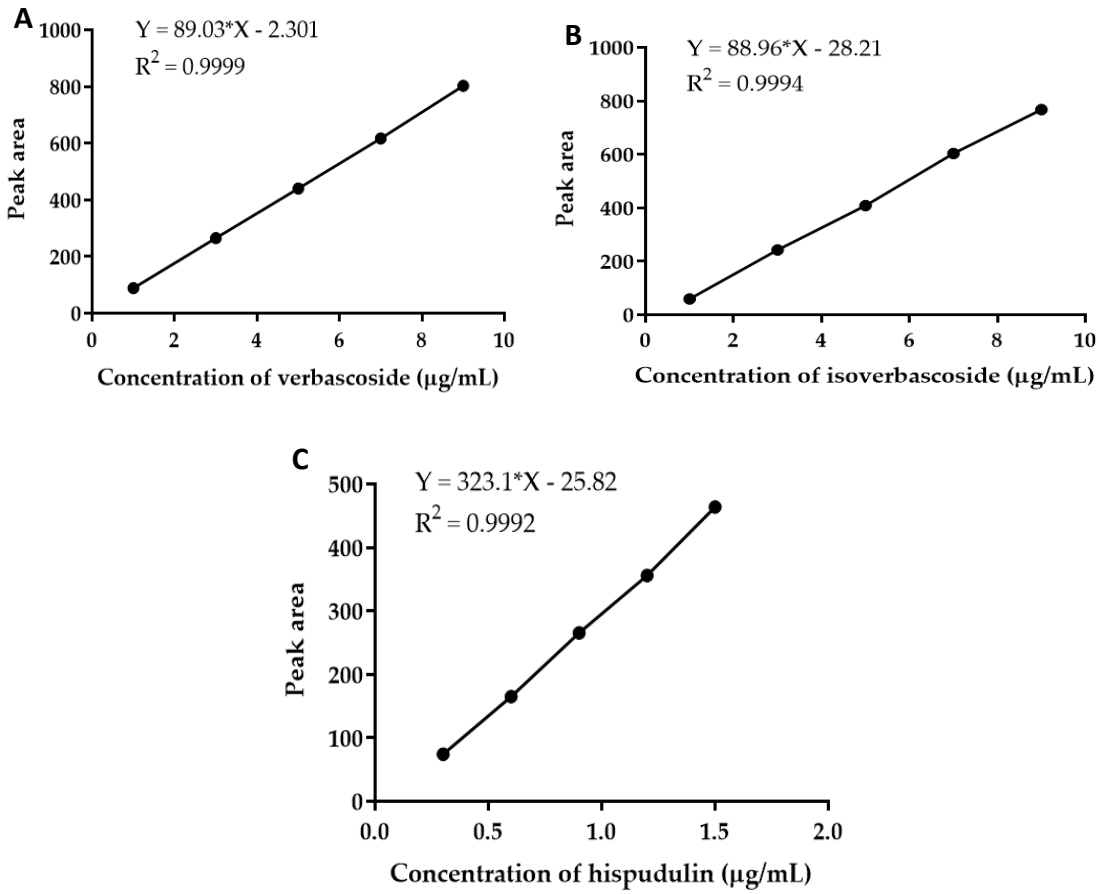

Figure 4. Calibration curve for peak area versus concentration of (A) verbascoside (B) isoverbascoside and (C) hispidulin

DPPH and ABTS free radical scavenging activity of *C. chinense* flower extract and NPs

The DPPH assay was used to determine and compare the free radical scavenging activities of *C. chinense* flower ethanolic extract and NPs. The % DPPH radical scavenging activities of quercetin, *C. chinensis* flower extract and NPs increased with concentration (Figure 5A). The concentration of quercetin, *C. chineses* flower extract and NPs that can inhibit 50% of the radical-scavenging effect (IC_{50} values) were 39.32, 482.9 and 660.9 µg/mL, respectively. The DPPH radical scavenging activity of *C. chinense* flower extract NPs was reduced to 95.95 ± 0.11% and 91.37 ± 0.70% after storing at 4°C for 1 and 2 months, respectively. It could be concluded that the nanoparticle of *C. chinense* flower extract can help protect the chemical compounds from degradation and control release of the bioactive compound (Zhang Yu et al., 2022).

ABTS free radical assay confirmed *C. chinense* flower extract's free radical scavenging activity. Quercetin and *C. chinense* flower extract demonstrated dose-dependent ABTS free radical scavenging activity (Figure 5B). The IC_{50} values of quercetin, *C. chinense* flower extract and NPs were 123.2, 1964 and 1613 µg/mL, respectively. The DPPH assay is based on the ability of hydrogen donor compounds to stabilize DPPH free radicals. In contrast, the ABTS assay

assesses the ability of samples to scavenge the radical cation produced by the oxidation of 2,2′-azinobis-3-ethylbenzothiazoline-6-sulphonate. As depicted in Figure 5, *C. chinense* flower extract (31.25-2,000 µg/mL and NPs (26.04-1,666.63 µg/mL) exhibited a dose-dependent DPPH and ABTS scavenging activities. The IC_{50} values of *C. chinense* flower extract and NPs suggested that the antioxidant activity of the extract was reduced when the extract was formulated in nanoparticulate form.

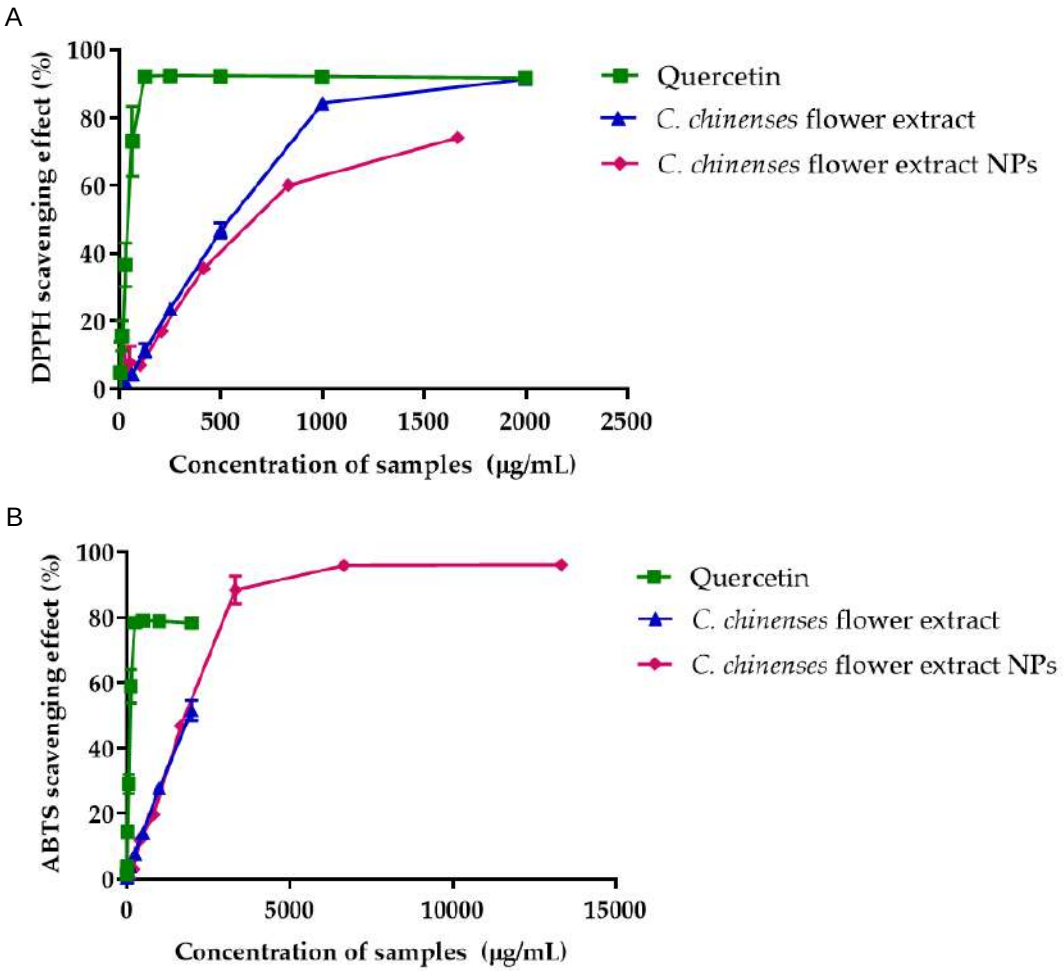

Figure 5. Antioxidant activity of quercetin, *C. chinense* flower ethanolic extract and NPs determined by (A) DPPH free radical scavenging assay and (B) ABTS free radical scavenging assay

FRAP of *C. chinense* flower extract and NPs

The FRAP values of quercetin, *C. chinense* flower extract and NPs, reported as Fe^{2+} equivalent, are illustrated in Figure 6. FRAP values of quercetin, *C. chinense* flower extract and NPs increased dose-dependently. FRAP values of quercetin, *C. chinense* flower extract and NPs were 154.29-2,461.44 µM, 88.73-2,480.81 µM, and 58.90 ± 1.80-2,448.08 ± 4.89 µM, respectively. These results suggested that the antioxidant activity of *C. chinense* extract and NPs involved ferric-reducing capacity.

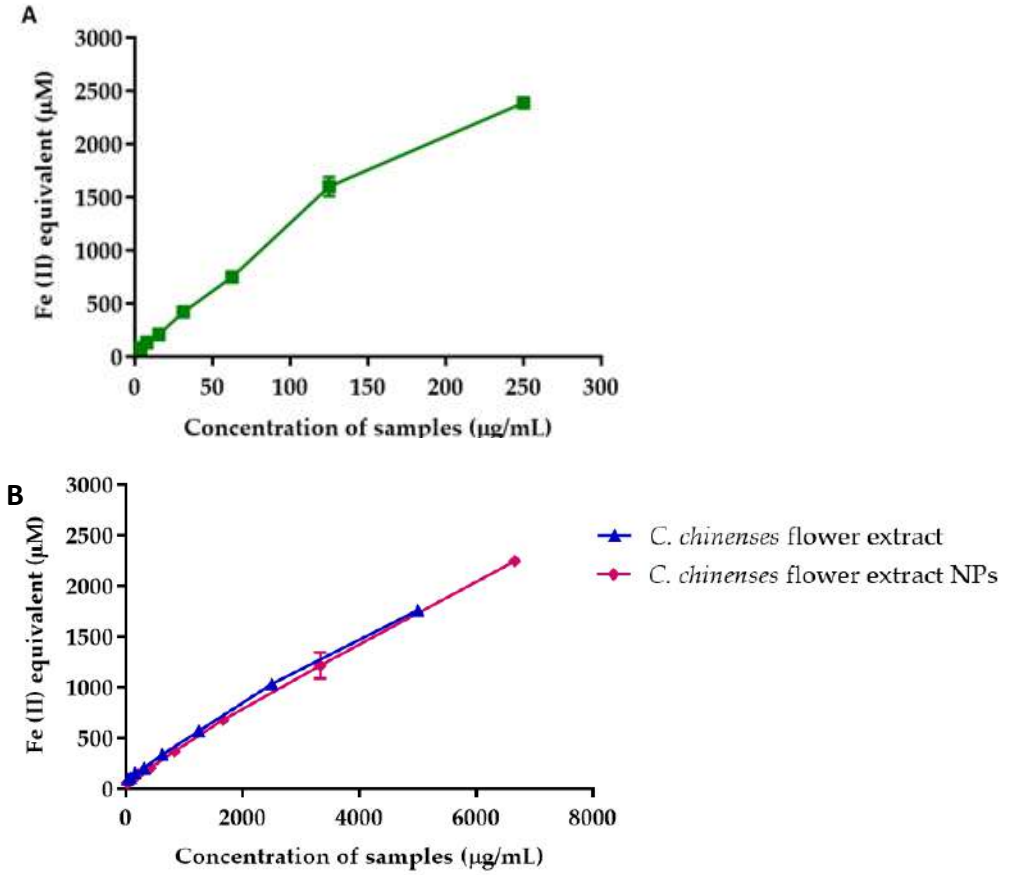

Figure 6. FRAP of (A) quercetin and (B) *C. chinense* flower extract and NPs

The FRAP assay is based on reducing a colorless ferric tripyridyltriazine (Fe^{3+}-TPTZ) complex into intense blue ferrous tripyridyltriazine (Fe^{2+}-TPTZ) once it interacts with a potent antioxidant. The structure-activity relationship (SAR) investigated by Spiegel et al. showed that compounds with two or more hydroxyl groups in ortho- or para-position to each other illustrated the highest antioxidant properties. Due to resonance stabilization, ortho-meta and para-meta hydroxylated phenolic acids have an improved activity over mono-hydroxylated ones and those having two hydroxyl groups in meta-position to each other. Verbascoside, isoverbascoside and hispidulin had para-meta hydroxylated phenolic acids, allowing them to have high activity in reducing ferric ions to ferrous ions (Spiegel et al., 2020).

Pearson correlation of total phenolic and flavonoid contents with antioxidant activity of *C. chineses* flower extract and NPs

The total phenolic and flavonoid content of *C. chinense* flower extract and NPs were correlated with its antioxidant activity by determining Pearson correlation coefficients. The antioxidant activities measured using the DPPH and ABTS assays were positively and significantly related to total phenolic and flavonoid content (Table 1). The FRAP assay revealed a strong relationship between ferric-reducing potential and total phenolic and flavonoid content.

Table 1. Pearson correlation coefficients of total phenolic and flavonoid contents and antioxidant activities of *C. chinense* flower ethanolic extract NPs measured by DPPH, ABTS and FRAP assays.

	Total Phenolic Content of extract (Gallic Acid Equivalent)	Total Flavonoid Content of extract (Quercetin Equivalent)	Total Phenolic Content of NPs (Gallic Acid Equivalent)	Total Flavonoid Content of NPs (Quercetin Equivalent)
DPPH assay	0.9033*	0.8371*	0.9549*	0.9302 *
ABTS assay	0.9995****	0.9528*	0.9980****	0.9988 ****
FRAP assay	0.9992****	0.9451*	0.9993****	0.9996 ****

Note: * Indicated $P < 0.05$ and **** indicated $P < 0.0001$.

Determination of cytotoxicity of *C. chinense* flower extract using sulforhodamine B (SRB) assay

The cytotoxicity assay was used to investigate the effect of *C. chinense* flower extract on cell metabolic activity. The cytotoxicity of *C. chinense* flower extract (0.025^{-1} mg/mL) was tested on A549, MCF-7 and HeLa cells 24 h, 48 h and 72 h after treatment. The cytotoxicity of *C. chinense* flower extract against HeLa, A549 and MCF-7 and cells were dose and time-dependent (Figure 7). The IC_{50} values of *C. chinense* flower extract against HeLa, A549 and MCF-7 cells at 24 h incubation were 369.2, 552 and 463.5 µg/mL, respectively. After 48 h, the IC_{50} values of *C. chinense* flower extract against HeLa, A549 and MCF-7 cells were reduced to 194.9, 285.6 and 178.6 µg/mL, respectively. After 72 h treatment, *C. chinense* flower extract decreased HeLa, A549 and MCF-7 cell viability with IC50 values of *C. chinense* flower extract of 155.1, 258.5 and 67.05 µg/mL, respectively. The IC_{50} values of *C. chinense* extract NPs were reported at >1,000 µg/mL and 668.8 µg/mL after treating with HeLa cells for 24-48 and 72 h, respectively. Interestingly, after 72 h incubation, the IC_{50} values of *C. chinense* flower extract were reduced up to 23.6 fold of the IC_{50} value of extract after 24-h incubation.

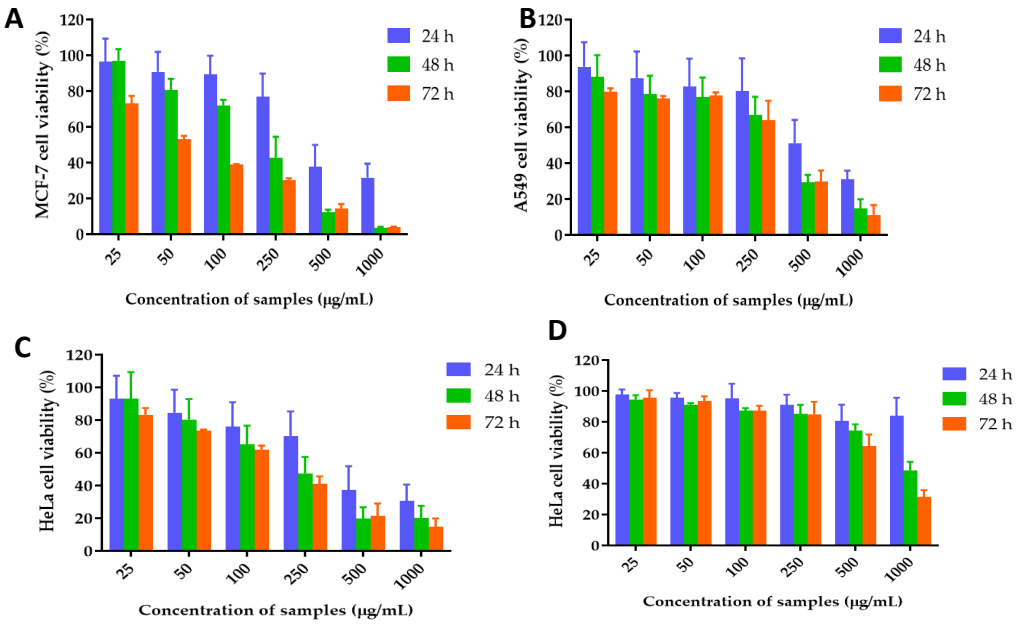

Figure 7. Effect of *C. chinense* flower extract on (A) MCF-7, (B) A549 and (C) HeLa cells after incubating 24, 48 and 72 h. (D) Effect of *C. chinense* flower extract NPs on HeLa cell viability after incubating for 24, 48 and 72 h. The data represented mean ± SD of three experiments.

AO/EB double-staining and fluorescent microscopy

A live/dead cell viability assay was performed to confirm the anticancer activities of *C. chinense* flower extract and NPs. Dual acridine orange/ethidium bromide (AO/EB) fluorescent staining can be used to identify apoptosis-associated changes of cell membranes during the process of apoptosis (Liu et al., 2015). This method can also accurately distinguish cells in different stages of apoptosis. Acridine Orange can cross the cell membrane of viable and early apoptotic cells. Ethidium Bromide is taken up by cells when cytoplasmic membrane integrity is lost. By visualizing or quantifying the relative proportions of green (live cells), red (late apoptotic and dead cells), and yellow (early apoptotic cells) fluorescence signals, it is possible to estimate the extent of apoptosis within the cell population (Atale et al., 2014; Fernando et al., 2015). Based on the cytotoxicity results, HeLa cell lines were treated with 100, 250 and 500 µg/ml of *C. chinense* flower extract and 250, 500 and 1,000 µg/ml of NPs. Dual staining was examined under a fluorescent microscope. No significant apoptosis was detected in the negative control group and cells treated with 100 µg/mL extract. As shown in Figure 8, bright yellow-green AO nuclear staining was observed in cells treated with 250 and 500 µg/mL extract and 250, 500 and 1,000 µg/mL NPs, indicating that the cells are at early-stage apoptosis. With increasing the concentrations (500 µg/mL of extract and 1,000 µg/mL of NPs), the number of late-stage apoptotic cells with localized orange nuclear EB staining was detected. AO penetrated normal and early apoptotic cells with intact membranes, fluorescing green when bound to DNA. EB only entered cells with damaged membranes, such as late apoptotic and dead cells, and emitted the orange-red fluorescence when bound to DNA fragments or apoptotic bodies (Liu et al., 2015).

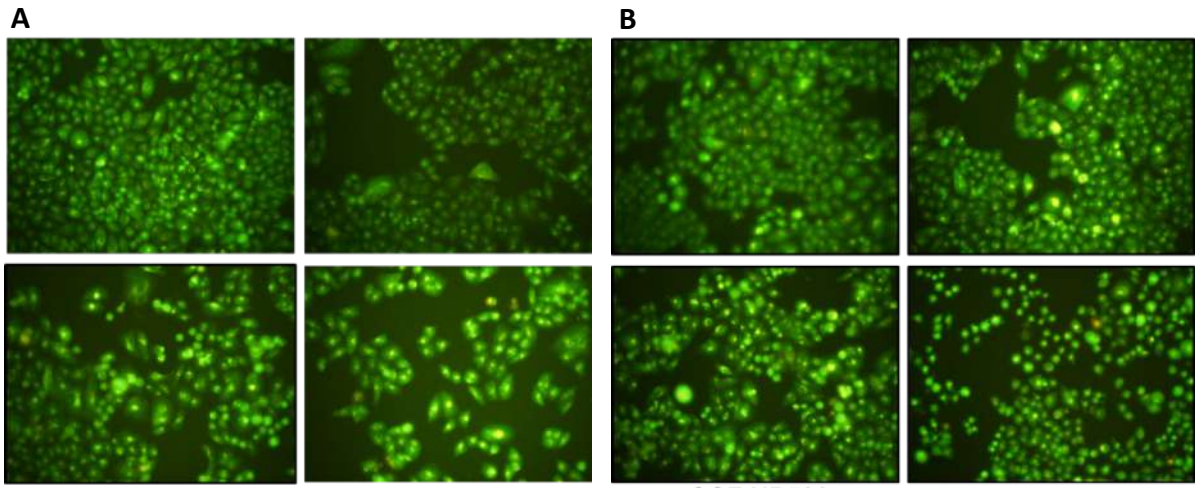

Figure 8. Apoptotic study with acridine orange/ethidium bromide double staining. Induction of apoptotic effect upon incubation of cells with different concentrations of (A) *C. chinense* flower extract and (B) *C. chinense* flower extract NPs on HeLa cells

C. chinense flower extract and NP-induced ROS generation in HeLa cells

The ROS levels in HeLa cells, treated with and without *C. chinense* flower extract and NPs, at different concentrations, were measured using the DCF-DA ROS detection assay kit. Flow cytometric analysis showed that the proportion of cells with higher fluorescent intensity was increased in cells after treating

with *C. chinense* flower extract and NPs in a concentration-dependent manner (Figure 9), indicating that the intracellular ROS in HeLa cells were significantly increased after treating with high concentrations of *C. chinense* flower extract and NPs. *C. chinense* flower extract at 500 µg/mL resulted in 3.90 ± 0.64% ROS formation compared with that of the control (1.50 ± 0.10%). *C. chinense* flower extract NPs at 500 and 1,000 µg/mL showed a significant increase in ROS production of 4.33 ± 0.46 and 7.20 ± 0.23%, respectively (Table 2).

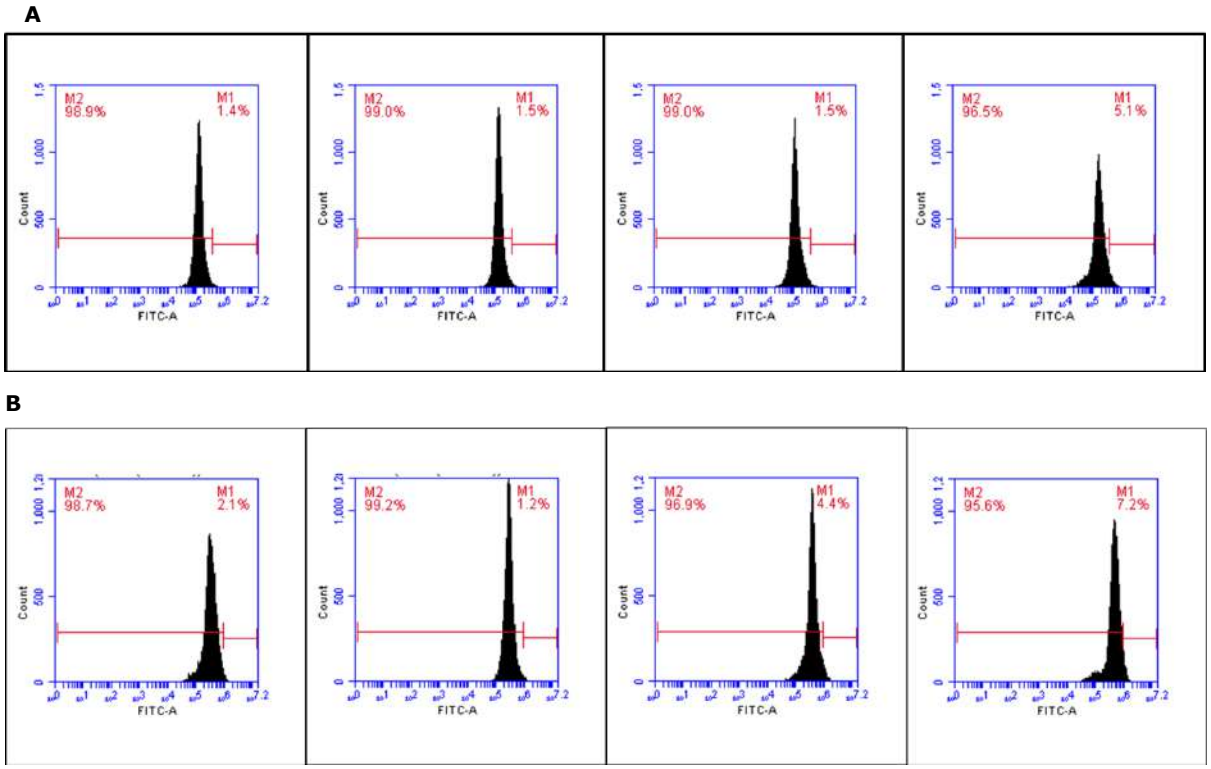

Figure 9. ROS formation percentage in (A) untreated HeLa cancer cells and HeLa cells treated with *C. chinense* flower extract at a concentration of 100, 250 and 500 µg/mL for 24 h, (B) untreated HeLa cancer cells and HeLa cells treated with *C. chinense* flower extract NPs at a concentration of 250, 500 and 1,000 µg/mL for 24 h and then labeled with DCF-DA (25 µM).

Table 2. Percentage of ROS formation of HeLa cells treated with various concentrations of *C. chinense* flower extract and NPs.

***C. chinense* flower extract**	**% ROS**	***C. chinense* flower extract NPs**	**% ROS**
0 µg/mL	1.50 ± 0.10	0 µg/mL	2.13 ± 0.32
100 µg/mL	1.37 ± 0.07	250 µg/mL	1.87 ± 0.77
250 µg/mL	1.50 ± 0.17	500 µg/mL	4.33 ± 0.46*
500 µg/mL	3.90 ± 0.64*	1000 µg/mL	7.20 ± 0.23*

Note: Results are shown as mean ± SD of three independent experiments with *P <0.05

C. chinense flower extract and NPs decreased HeLa cancer cell colony formation.

The colony-forming assay measures the ability of individual cells to form colonies and proliferate, indicating their clonogenic potential. Clonogenic survival is a critical characteristic of cancer cells, as it represents their capacity

to survive and form new tumors (Fedr et al., 2013; Rajendran V. et al., 2018). The number and size of colonies formed were quantified to assess the impact of *C. chinense* flower extract nanoparticles on the survival and growth of HeLa cells. The clonogenic formation potential of HeLa cells was evaluated as a function of a number of colony formations in the absence or presence of *C. chinense* flower extract and NPs at various concentrations. The results showed that *C. chinense* flower extract and NPs significantly suppressed the clonogenic formation of HeLa cells. The number of colonies of HeLa cells significantly decreased after treating with *C. chinense* flower extract and NPs in a dose-dependent manner (Figure 10). HeLa cells formed 100 ± 11.10% without treatment. HeLa cells treated with 25, 50, 100 and 250 µg/mL *C. chinense* flower extract showed 90.10 ± 38.13, 114.67 ± 7.73, 58.70 ± 6.97 and 38.57 ± 5.25% colony formation, respectively, compared with control. HeLa cells treated with 50, 100, 250 and 500 µg/mL *C. chinense* flower extract NPs showed 52.49 ± 6.93, 27.20 ± 7.39, 4.60 ± 1.99 and 1.15 ± 1.15% colony formation, respectively, compared with control. Cells exposed to 500 µg/mL *C. chinense* flower extract and 1,000 µg/mL *C. chinense* flower extract NPs did not form colonies.

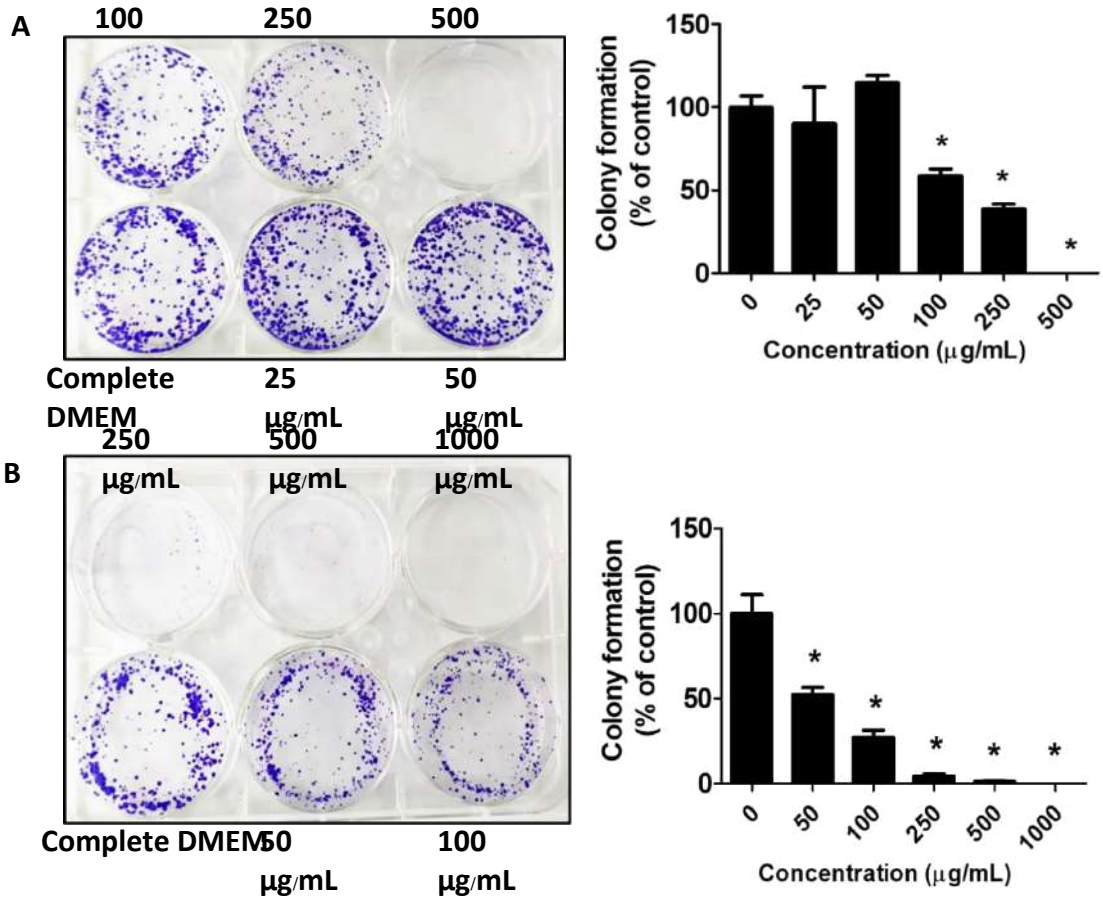

Figure 10. Clonogenic formation of HeLa cells treated with (A) 0, 25, 50, 100, 250 and 500 µg/mL of *C. chinense* flower extract (B) 0, 50, 100, 250, 500 and 1000 µg/mL of *C. chinense* flower extract NPs. Results are shown as mean ± SD of three independent experiments with **P* <0.05.

C. chinense flower extract and NPs induced cell cycle arrest at different phases in HeLa cells

Effects of *C. chinense* flower extract and NPs on cell cycle distribution in HeLa cells are presented in Figure 11. The cell cycle distribution of HeLa cells was analyzed using flow cytometry. The proportions of HeLa cells in G0/G1 phases, S phases and G2/M phases are shown in the histograms. Compared with the control group, HeLa cells treated with *C. chinense* flower extract (250 µg/mL) induced cell cycle arrest at the G2/M phase (Figure 12A). The proportion of HeLa cells treated with 250 and 500 µg/mL of *C. chinense* flower extract NPs induced cell cycle arrest at the G0/G1 and S phase, while 1000 µg/mL arrested the cell cycle at the G2/M phase (Figure 12B). Accordingly, the proportions of HeLa cells treated with NPs in the G0/G1 phase decreased.

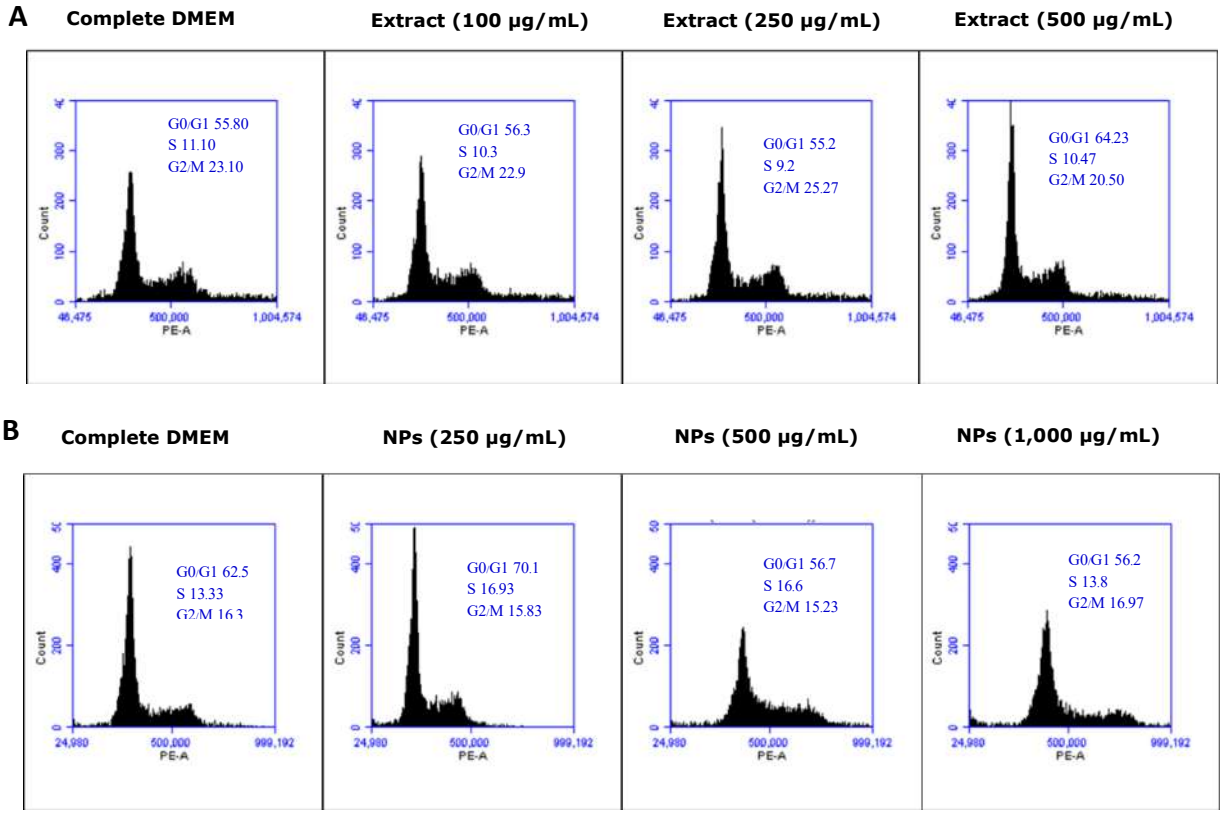

Figure 11. Cell cycle arrest of HeLa cells treated with (A) 0, 100, 250 and 500 µg/mL of *C. chinense* flower extract and (B) 0, 250, 500 and 1,000 µg/mL of *C. chinense* flower extract NPs.

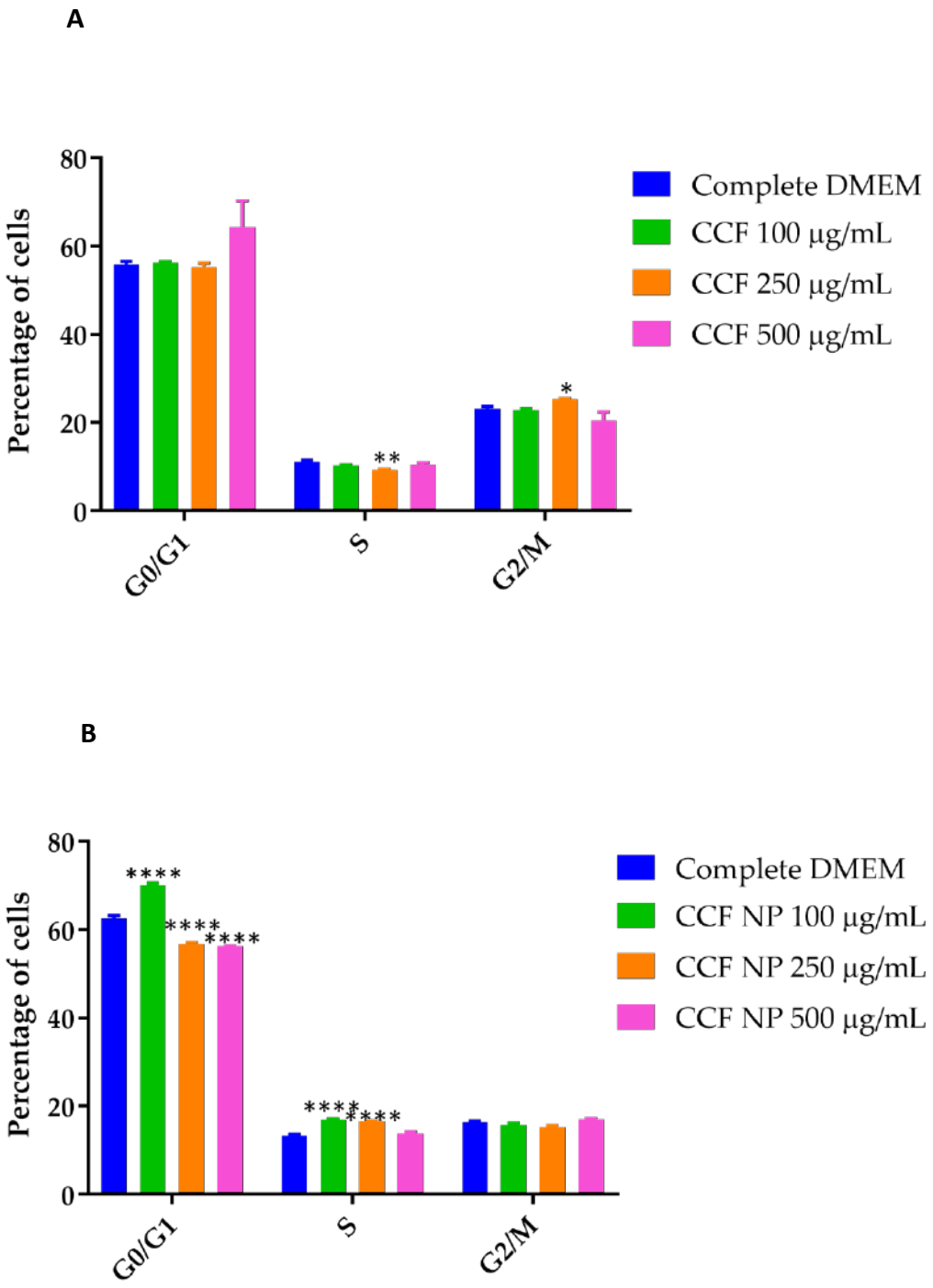

Figure 12. Plots of cell cycle arrest induced by different concentrations of (A) *C. chinense* flower extract and (B) *C. chinense* flower extract NPs. Results are shown as mean ± SD of three independent experiments with **P* <0.05, ***P* <0.01, and *****P* <0.0001.

DISCUSSION

Extraction is a primary process for isolating various bioactive secondary metabolites from plant materials. In this study, 95% ethanol was used for maceration to extract polar compounds from *C. chinense* flower because it employs an eco-friendly process, low toxicity, and possesses high polarity compared with other nonpolar solvents. Sapiun et al. reported that the yield obtained from extracting *C. chinense* flower was equal to 7.6% (Zulfiayu et al., 2020). The higher yield of extraction observed in this study might have been due to the optimal ratio between plant and solvent, which was 1:10. We are the first to report the total phenolic and flavonoid contents in *C. chinense* flower ethanolic extract. Kopilakkal et al. revealed that the total phenolic and total flavonoid contents in the alcoholic extract of *C. paniculatum* flower were 393.23 ± 1.23 mg GAW/g and 378.5 ± 0.883 mg QE/g, respectively. The results suggested that *C. chinense* flower contained a higher amount of total phenolic compounds but lower total flavonoid contents than *C. paniculatum* (Kopilakkal et al., 2021). Compared with other parts of the plant, the total flavonoid content in the leaf of *C. chinense* was 134.79 mg QE per g of dry extract (Zulfiayu et al., 2020). Wong and Tan analyzed the volatile constituents of *C. chinense* flower extract by GC-MS and identified oxygenated monoterpenes and aromatic compounds as the most predominant of the total volatiles (Wong et al., 2005).

The nano-sized delivery system is a potential and promising strategy for targeting cancer therapy. The solvent displacement method did not require the shear stress or high energy to produce NPs. The NPs were formed by taking advantage of Marangoni effect, where ethanol rapidly diffused out of the nanodroplets due to the differences in the interfacial tension between ethanol and water (Ahlin Grabnar et al., 2011). *C. chinense* flower extract then precipitated in the form of nanoparticles (Lepeltier et al., 2014). The surface of the NPs was coated with surfactant which increased NP colloidal stability by preventing aggregation (Shubhra et al., 2014). Poloxamer 407 can stabilize the ethanolic extract of *C. chinense* flower in an aqueous medium, allowing the possibility to encapsulate an extract and form nanoparticles. Poloxamer 407 is a triblock copolymer consisting of polyethylene oxide (PEO) – polypropylene oxide (PPO)- PEO. The inner core of polymeric micelles constituting hydrophobic blocks (PPO) adhered to the hydrophobic part of the extract, whereas the hydrophilic chain (PEO) formed the hydrophilic corona (Almeida et al., 2017). The hydrophobic core can serve as an extract-loading site, allowing for the encapsulation of *C. chinense* flower extract via physical or chemical interactions. The nanoparticle size, PDI, and zeta potential values were all within acceptable limits, indicating that the solvent displacement method successfully created nanoparticles. The results showed that the polydispersity index and zeta potential values of the NPs did not change significantly after up to six months of storing at 4°C. The size of NPs was significantly larger than freshly prepared NPs after storing at 4°C for four months. Therefore, these results suggested that *C. chinense* flower extract should be stored for up to two months at 4°C.

The negative surface charge of *C. chinense* flower extract NPs resulted from the polyphenolic compounds, containing free carboxylic groups that can dissociate in an aqueous medium (Saxena et al., 2012). The stability study showed that at high temperatures (45°C), the NPs had significantly lower negative zeta potential values within a month of storage. The increase in positive zeta potential value upon an increase in temperature agreed with Freitas et al who reported that poloxamer 188 stabilizing solid lipid dispersion showed a decreased in zeta potential after storage at higher temperature (50°C). The zeta potential decreases in increasing energy input from increasing

temperature (Freitas et al., 1998). According to the DLVO theory, the magnitude of the zeta potential indicates the potential stability of the colloidal system. The NPs should be stable if they possess large zeta potential (> ± 30 mV) when the electrostatic repulsion dominates the attractive van der Waals force (Gumustas et al., 2017). Storage of NPs at higher temperatures increases the kinetic energy of the system and leads to the collision of the NPs (Freitas et al., 1998). If the particles in dispersion have zeta potential close to zero, the NPs that had low negative zeta potential values may aggregate and precipitate. Poloxamer stabilized *C. chinense* flower extract NPs, presumably because the hydrophilic part of the tri-block copolymer extended toward the bulk solution. In contrast, the insoluble part adhered to the NPs' surface due to hydrophobic interaction. In addition, when surrounded by a layer of electric charges, NPs are stabilized by the repulsive electrostatic force. Generally, the nanoparticles with poloxamer completely attached to the surface remained in the colloidal solution, while the low negative charge can lead to nanoparticle precipitation. However, we did not observe precipitation in our stability study.

Pearson correlation coefficient measures the strength of a linear association between two variables and is denoted by r. Pearson correlation coefficient suggested that the antioxidant activity of *C. chinense* flower extract and NPs evaluated by DPPH, ABTS and FRAP assays correlated with total phenolic and total flavonoid levels, mainly due to the hydrogen atom donation and redox properties of phenolic compounds. Table 1 demonstrates that the DPPH and ABTS scavenging activities of *C. chinense* flower extract and NPs significantly correlated with TPC and TFC. Formulating extract into nanoparticles did not affect the phenolic and flavonoid contents of *C. chinense* flower extract. However, the antioxidant activity of the NPs was reduced compared with the extract, which might have resulted from the encapsulation of the extract inside the core, sustaining the release of the extract.

Herein, the cytotoxicity of *C. chinense* flower extract against HeLa, A549 and MCF-7 cell lines was first reported. The results showed the strongest cytotoxicity against HeLa cervical cancer cells, followed by MCF-7 breast cancer cells and A549 lung cancer cells, after 24 h incubation. After 48 and 72 h incubation, the IC_{50} values of *C. chinense* flower extract on all cancer cell lines decreased with the incubation time, indicating that all cancer cells could not tolerate the extract at 25 to 1,000 µg/mL concentration range. The antiproliferative effect of *C. chinense* flower extract NPs was evaluated against HeLa cells to confirm the alternative for anticervical cancer therapy. The IC_{50} values of *C. chinense* extract NPs were reported at >1,000 µg/mL and 668.8 µg/mL after treating with HeLa cells for 24-48 h, and 72 h, respectively. Interestingly, after 72 h incubation, the IC_{50} values of *C. chinense* flower extract were reduced up to 23.6 fold of the IC_{50} value of extract after 24 h-incubation. The unloaded nanoparticles were composed of poloxamer 407, used as a surfactant/stabilizer of the nanoparticles. It was reported that poloxamer 407 at 0.1% w/w was non-cytotoxic and safe to use in animals (Singh-Joy et al., 2008; Querobino et al., 2019; Vigani et al., 2019). Conjugation of poloxamer 407 with other cytotoxic polymer reduced toxicity of other polymer against HeLa cells (Shu et al., 2019).

C. chinense flower extract exhibited the IC_{50} values of 369.2, 194.9, and 155.1 µg/mL after 24-incubation to HeLa cells for 24, 48, and 72 h. Previous studies showed that paclitaxel and carboplatin, chemotherapeutic drugs, had IC_{50} values of 112.53 and 323.57 µg/mL, respectively. The IC_{50} value of gallic acid against HeLa cells was 1.95 mg/mL (Aborehab et al., 2019). The result suggested that the extract had higher IC_{50} values than that of chemotherapeutic drugs. But it showed higher toxicity to HeLa cells when compared with gallic acid. For the same genus plant, it was found that the IC_{50} value of *Clerodendrum viscosum* methanolic leaf extract against HeLa cells was 831.93 µg/mL (Shendge et al., 2021).

Antioxidants are typically known for their ability to protect cells from oxidative damage by neutralizing reactive oxygen species (ROS). However, some antioxidants can promote the production of ROS, which is referred to as their pro-oxidant activity. There are several reasons that certain antioxidants exhibit pro-oxidant effects. Firstly, the concentration and dose of antioxidants play a role. At low concentrations, antioxidants act by scavenging ROS, but at higher concentrations, they can generate ROS. This shift in activity may be due to altering the complex system of endogenous antioxidative defense of cells or altering the cell apoptosis pathways at higher antioxidant concentrations (Poljsak et al., 2013). Environmental factors also play a role in the pro-oxidant activity of antioxidants. For instance, antioxidants stable in neutral pH environments may become reactive in acidic conditions or in the presence of specific enzymes (Bayliak et al., 2016). These altered conditions can trigger the antioxidants to produce ROS. Furthermore, some antioxidants, such as quinones, can undergo redox cycling, leading to the generation of ROS as byproducts (Rajashekar, 2023). This process involves repeated cycles of oxidation and reduction, which can cause oxidative damage to cells. The cytotoxicity of *C. chinense* flower extract possibly results from polyphenols in the extract including verbascoside, isoverbascoside and hispidulin. Vo et al. reported the strong cytotoxic activity of verbascoside and isoverbascoside against the MCF-7 breast cancer cell line (Vo et al., 2012). The cytotoxic effects of pure verbascoside isolated from *Phlomis nissolinii* L. plant were observed in both MCF-7 and MDA-MB-231 cell lines (Şenol et al., 2021). Verbascoside effectively inhibited OSCC tumor cell growth and metastasis by suppressing the IκB kinase complex (IKK)/NF-κB-related signaling activation (Zhang Y. et al., 2018). Verbascoside inhibits the proliferation of 4 T1 cancer cells (IC_{50} 117 μM) while remaining safe for normal cells. It induces apoptosis in 4 T1 cells through the TLR4 axis (Daneshforouz et al., 2021). Verbascoside also exhibited potential antitumor activities in leukemia. The verbascoside treatment significantly decreased the Tyr-412 phosphorylation of Abl in K562 and R-K562 cells. The antileukemic mechanisms of verbascoside may be mediated by the Abl protein and regulation of its downstream p38-MAPK/JNK pathway, caspase-3 and oxidative stress in CML cells (Akgun-Cagliyan et al., 2022). The antiproliferation activity of verbascoside in breast cancer cells may be associated with cell cycle arrest and apoptosis. Verbascoside treatment altered the expression of cell cycle and apoptosis-related proteins and suppressed the activity of the PI3K/AKT signaling pathway (Ou et al., 2022). Isoverbascoside also inhibited cell proliferation and caused differentiation in MGC 803 cells, which might have been associated with G0/G1 arrest and regulating the expression of cell cycle related proteins (Chen R. C. et al., 2002).

C. chinense flower extract at 500 μg/mL resulted in 3.90 ± 0.64% ROS formation compared with the control (1.50 ± 0.10%). *C. chinense* flower extract NPs at 500 and 1,000 μg/mL showed a significant increase in ROS production of 4.33 ± 0.46% and 7.20 ± 0.23%, respectively. We previously reported that *C. chinense* leaf extract at 250 μg/mL induced 15.95 ± 3.95% ROS formation, compared with control (2.22 ± 0.59%) (Chittasupho C. et al., 2023b). Because redox balance of intracellular ROS levels is required for tumor development and progression, one strategy for cancer therapy is to elevate oxidative stress to stimulate ROS formation. Increased ROS production has been linked to cancer cell apoptosis and cell cycle arrest. Our results showed that *C. chinense* flower extract (500 μg/mL) and the NPs (500 and 1,000 μg/mL) significantly increased ROS formation compared with untreated cells. Excessive cellular ROS levels damage proteins, nucleic acids, lipids, membranes and organelles, activating cell death processes such as apoptosis. ROS is important in cell signaling and regulating the main apoptosis pathways mediated by mitochondria, death receptors, and the endoplasmic reticulum (Redza-Dutordoir et al., 2016).

The inhibition of cancer cell colony formation of *C. chinense* extract and NPs confirmed the proliferation suppression of HeLa cells, which might have been mainly caused by verbascoside and isoverbascoside. Verbascoside induces cell cycle arrest in MCF-7 and MDA-MB-231 breast cancer cell lines by suppressing the expression of Cdc2 and cyclinB1, which are the main mediators in controlling G2 phase progression and G2/M phase transition (Ou et al., 2022). In another study, verbascoside inhibited cell proliferation and colony formation of three hepatocarcinoma cell lines, including BEL7404, HLF and JHH-7 (Ma et al., 2020). Attia et al. reported that verbascoside inhibited the proliferation of CaCo-2 and HCT-116 cells by inducing G0/G1 phase arrest (Attia et al., 2018). Isoverbascoside induced G0/G1 arresting of hepatocellular carcinoma SMMC-7721 cell lines (Rui-Chuan et al., 2002).

The mechanism of cell cycle arrest induction varies between different cell types or drugs and different concentrations of the same drug, compound or drug addiction at different phases of the cell cycle (Sakaue-Sawano et al., 2011). Cell cycle arrest at different phases by the same anticancer drug has been reported. Etoposide at different concentrations resulted in NMuMG cell cycle arrest at different phases (Sakaue-Sawano et al., 2011). Different concentrations of Cisplatin also halted the HL-60 cell cycle at different phases. At lower doses of Cisplatin treatment, the cells were arrested at sub-G1, S or G2 checkpoints, and as Cisplatin dose and treatment time increased, the cells started accumulating more in the sub-G1 phase (Velma et al., 2016). Foscarnet showed different phases of embryonic fibroblast cell cycle arrest at different concentrations and incubation times. At a low dose of foscarnet, the G2 phase was markedly affected, while at a higher dose, the cell cycle was greatly reduced in the G1 and S phases (Stenberg et al., 1985). Therefore, we conclude that the cytotoxicity and antiproliferative effect of *C. chinense* flower extract and NPs were related to apoptosis induction, ROS formation, colony-forming inhibition and cell cycle arrest. The NPs containing *C. chinense* flower extract were useful as chemotherapeutic agents for cervical cancer cells. The specificity of extract and NPs must be determined by *in vivo* studies. Conjugating the targeting ligands such as peptides, antibodies, small molecules or oligonucleotides may provide a promising strategy to deliver the nanoparticles encapsulating extract to cancer cells specifically (Chittasupho et al., 2010; Chittasupho et al., 2014).

CONCLUSION

C. chinense flower extract contained verbascoside and isoverbascoside (phenolic compound) and hispidulin (flavonoid). The extract showed antioxidant activities related to its phenolic and flavonoid contents. Verbascoside, isoverbascoside and hispidulin were detected in this extract. *C. chinense* flower extract exhibited dose-dependent cytotoxicity against MCF-7, A549 and HeLa cancer cells. The nanoparticles of *C. chinense* flower extract and the extracts exhibited cell apoptosis induction, inducing ROS formation, decreasing colony formation and stimulating cell cycle arrest against HeLa cervical cancer cells. NPs containing *C. chinense* flower extract are appropriate for use as a drug delivery system. These findings suggest that *C. chinense* flower extract and NPs might constitute a potential leading candidate for developing chemotherapeutic agents against cancer.

ACKNOWLEDGMENTS

This work was supported by the Faculty of Pharmacy, Srinakharinwirot University (Grant No. 236/2565) and partially supported by Chiang Mai University.

AUTHOR CONTRIBUTIONS

Conceptualization, C.C. (Chuda Chittasupho) and S.A. (Sirivan Athikomkulchai); methodology, C.C., W.S. (Weerasak Samee), W.J. (Wullapa Jittachai), and S.A.; formal analysis, C.C., S.T. (Sarin Tadtong), and C.M. (Chittima Managit); investigation, C.C., W.S., W.J., and S.A.; writing—original draft preparation, C.C.; writing—review and editing, C.C., W.S., S.T., W.J., C.M., and S.A. All authors have read and agreed to the published version of the manuscript.

CONFLICT OF INTEREST

The authors declare that they hold no competing interests.

REFERENCES

Aborehab N.M., Osama N. 2019. Effect of gallic acid in potentiating chemotherapeutic effect of paclitaxel in hela cervical cancer cells. Cancer Cell International. 19: 154.

Abouzid S.F., Wahba H.M., Elshamy A., Cos P., Maes L., Apers S., Pieters L., and Shahat A.A. 2013. Antimicrobial activity of some *Clerodendrum* species from egypt. Natural Product Research. 27(11): 1032-1036.

Ahlin Grabnar P. and Kristl J. 2011. The manufacturing techniques of drug-loaded polymeric nanoparticles from preformed polymers. Journal of Microencapsulation. 28(4): 323-335.

Akgun-Cagliyan G., Cort-Donmez A., Kilic-Toprak E., and Altintas F. 2022. Verbascoside potentiates the effect of tyrosine kinase inhibitors on the induction of apoptosis and oxidative stress via the abl-mediated mapk signalling pathway in chronic myeloid leukaemia. Experimental and Therapeutic Medicine. 24(2): 514.

Almeida M., Magalhães M., Veiga F., and Figueiras A. 2017. Poloxamers, poloxamines and polymeric micelles: Definition, structure and therapeutic applications in cancer. Journal of Polymer Research. 25(1): 31.

Atale N., Gupta S., Yadav U.C., and Rani V. 2014. Cell-death assessment by fluorescent and nonfluorescent cytosolic and nuclear staining techniques. Journal of Microscopy. 255(1): 7-19.

Attia Y.M., El-Kersh D.M., Wagdy H.A., and Elmazar M.M. 2018. Verbascoside: Identification, quantification, and potential sensitization of colorectal cancer cells to 5-fu by targeting pi3k/akt pathway. Scientific Reports. 8(1): 16939.

Barung E.N., Kalonio D.E., Banne Y., and Kambuno N.T. 2021. Anticancer activities of sesewanua leaf extracts (*Clerodendrum fragrans* (vent.) willd) against a549 lung cancer cell. Macedonian Journal of Medical Sciences. 9(A): 1226-1230.

Bayliak M., Burdyliuk N., and Lushchak V. 2016. Effects of pH on antioxidant and prooxidant properties of common medicinal herbs. Open Life Sciences. 11: 298-307.

Buranasukhon W., Athikomkulchai S., Tadtong S., and Chittasupho C. 2017. Wound healing activity of *Pluchea indica* leaf extract in oral mucosal cell line and oral spray formulation containing nanoparticles of the extract. Pharmaceutical Biology. 55(1): 1767-1774.

Chen P.M., Yung L.L., Hsiao K.I., Chen C.M., Yeh H.M., Chuang M.H., and Tzeng C.H. 1988. *In vitro* induction of differentiation in hl-60 leukemic cell line by *Clerodendron fragrans*. American Journal of Chinese Medicine. 16(3-4): 139-144.

Chen R.C., Su J.H., Yang S.M., Li J., Wang T.J., and Zhou H. 2002. Effect of isoverbascoside, a phenylpropanoid glycoside antioxidant, on proliferation and differentiation of human gastric cancer cell. Acta Pharmacologica Sinica. 23(11): 997-1001.

Chiangnoon R., Samee W., Uttayarat P., Jittachai W., Ruksiriwanich W., Sommano S.R., Athikomkulchai S., and Chittasupho C. 2022. Phytochemical analysis, antioxidant, and wound healing activity of *Pluchea indica* L. (less) branch extract nanoparticles. Molecules. 27(3): 635.

Chittasupho C. and Athikomkulchai S. 2018. Nanoparticles of *Combretum quadrangulare* leaf extract induce cytotoxicity, apoptosis, cell cycle arrest and anti-migration in lung cancer cells. Journal of Drug Delivery Science and Technology. 45: 378-387.

Chittasupho C., Athikomkulchai S., Samee W., Na Takuathung M., Yooin W., Sawangrat K., and Saenjum C. 2023a. Phenylethanoid glycoside-enriched extract prepared from *Clerodendrum chinense* leaf inhibits a549 lung cancer cell migration and apoptosis induction through enhancing ros production. Antioxidants. 12(2): 461.

Chittasupho C., Athikomkulchai S., Samee W., Na Takuathung M., Yooin W., Sawangrat K., and Saenjum C. 2023b. Phenylethanoid glycoside-enriched extract prepared from *Clerodendrum chinense* leaf inhibits a549 lung cancer cell migration and apoptosis induction through enhancing ros production. Antioxidants. 12(2): 461.

Chittasupho C., Manikwar P., Krise J.P., Siahaan T.J., and Berkland C. 2010. Cibr effectively targets nanoparticles to LFA-1 on acute lymphoblastic T cells. Molecular Pharmaceutics. 7(1): 146-155.

Chittasupho C., Sestak J., Shannon L., Siahaan T.J., Vines C.M., and Berkland C. 2014. Hyaluronic acid graft polymers displaying peptide antigen modulate dendritic cell response *in vitro*. Molecular Pharmaceutics. 11(1): 367-373.

Daneshforouz A., Nazemi S., Gholami O., Kafami M., Amin B. 2021. The cytotoxicity and apoptotic effects of verbascoside on breast cancer 4t1 cell line. BMC Pharmacology and Toxicology. 22(1): 72.

Fedr R., Pernicová Z., Slabáková E., Straková N., Bouchal J., Grepl M., Kozubík A., and Souček K. 2013. Automatic cell cloning assay for determining the clonogenic capacity of cancer and cancer stem-like cells. Cytometry Part A. 83A(5): 472-482.

Fernando D.M., Wijesundera R.L.C., Soysa P., de Silva D., and Nanayakkara C.M. 2015. Antioxidant potential, *in vitro* cytotoxicity and apoptotic effect induced by crude organic extract of *Anthracophyllum lateritium* against rd sarcoma cells. BMC Complementary and Alternative Medicine. 15(1): 398.

Freitas C. and Müller R.H. 1998. Effect of light and temperature on zeta potential and physical stability in solid lipid nanoparticle (sln™) dispersions. International Journal of Pharmaceutics. 168(2): 221-229.

Gavas S., Quazi S., and Karpiński T.M. 2021. Nanoparticles for cancer therapy: Current progress and challenges. Nanoscale Research Letters. 16(1): 173.

Gumustas M., Sengel-Turk C.T., Gumustas A., Ozkan S.A., and Uslu B. 2017. Chapter 5 - Effect of polymer-based nanoparticles on the assay of antimicrobial drug delivery systems. p. 67-108. In: A.M. Grumezescu (ed). Multifunctional systems for combined delivery, biosensing and diagnostics. Elsevier.

Kopilakkal R., Chanda K., and Balamurali M.M. 2021. Hepatoprotective and antioxidant capacity of *Clerodendrum paniculatum* flower extracts against carbon tetrachloride-induced hepatotoxicity in rats. ACS Omega. 6(40): 26489-26498.

Lepeltier E., Bourgaux C., and Couvreur P. 2014. Nanoprecipitation and the "ouzo effect": Application to drug delivery devices. Advanced Drug Delivery Reviews. 71: 86-97.

Liu K., Liu P.C., Liu R., and Wu X. 2015. Dual ao/eb staining to detect apoptosis in osteosarcoma cells compared with flow cytometry. Medical Science Monitor Basic Research. 21: 15-20.

Ma D., Wang J., Liu L., Chen M., and Wang Z. 2020. Acteoside as a potential therapeutic option for primary hepatocellular carcinoma: A preclinical study. BMC Cancer. 20(1): 936.

Mileo A.M. and Miccadei S. 2016. Polyphenols as modulator of oxidative stress in cancer disease: New therapeutic strategies. Oxidative Medicine and Cellular Longevity. 2016: 6475624.

Ou Y., Zhang Y., Zhu X., and Zhu D. 2022. Verbascoside induces the cell cycle arrest and apoptosis of breast cancer *via* suppression of the pi3k/akt signaling pathway. Research Square. April 13th , 2022: 1-13

Poljsak B., Šuput D., and Milisav I. 2013. Achieving the balance between ros and antioxidants: When to use the synthetic antioxidants. Oxidative Medicine and Cellular Longevity. 2013: 956792.

Qi J., Zhang Y., Liu Q., Liu H., Fan Y., and Yue J. 2021. Clerodenoids a—f: C-ring aromatized and/or rearranged abietane diterpenoids from *Clerodendrum chinense* var. Simplex. Chinese Journal of Chemistry. 39(7): 1891-1897.

Querobino S.M., de Faria N.C., Vigato A.A., da Silva B.G.M., Machado I.P., Costa M.S., Costa F.N., de Araujo D.R., Alberto-Silva C. 2019. Sodium alginate in oil-poloxamer organogels for intravaginal drug delivery: Influence on structural parameters, drug release mechanisms, cytotoxicity and *in vitro* antifungal activity. Materials Science and Engineering: C 99:1350-1361.

Rajashekar C. 2023. Dual role of plant phenolic compounds as antioxidants and prooxidants. American Journal of Plant Sciences. 14: 15-28.

Rajendran P., Abdelsalam S.A., Renu K., Veeraraghavan V., Ben Ammar R., and Ahmed E.A. 2022. Polyphenols as potent epigenetics agents for cancer. International Journal of Molecular Sciences. 23(19): 11712.

Rajendran V. and Jain M.V. 2018. *In vitro* tumorigenic assay: Colony forming assay for cancer stem cells. Methods in Molecular Biology. 1692: 89-95.

Redza-Dutordoir M. and Averill-Bates D.A. 2016. Activation of apoptosis signalling pathways by reactive oxygen species. Biochimica et Biophysica Acta (BBA) - Molecular Cell Research. 1863(12): 2977-2992.

Reuter S., Gupta S.C., Chaturvedi M.M., and Aggarwal B.B. 2010. Oxidative stress, inflammation, and cancer: How are they linked? Free Radical Biology and Medicine. 49(11): 1603-1616.

Rui-Chuan C., Jin-Hua S., Gao-Liang O., Ke-Xia C., Jin-Quan L., and Xiao-Guang X. 2002. Induction of differentiation in human hepatocarcinoma cells by isoverbascoside. Planta Medica. 68(4): 370-372.

Sakaue-Sawano A., Kobayashi T., Ohtawa K., and Miyawaki A. 2011. Drug-induced cell cycle modulation leading to cell-cycle arrest, nuclear mis-segregation, or endoreplication. BMC Molecular and Cell Biology. 12: 2.

Saxena V. and Hussain M.D. 2012. Poloxamer 407/tpgs mixed micelles for delivery of gambogic acid to breast and multidrug-resistant cancer. International Journal of Nanomedicine. 7: 713-721.

Şenol H., Tulay P., Ergören M., Hanoğlu A., Çalış İ., and Mocan G. 2021. Cytotoxic effects of verbascoside on mcf-7 and mda-mb-231. Turkish Journal of Pharmaceutical Sciences. 18(5): 637-644.

Shendge A.K., Basu T., and Mandal N. 2021. Evaluation of anticancer activity of *Clerodendrum viscosum* leaves against breast carcinoma. Indian Journal of Pharmacology. 53(5): 377-383.

Shu H., Zhang Y., Zhang M., Wu J., Cui M., Liu K., and Wang J. 2019. Addition of free poloxamer 407 to a new gene vector p407-pei-k12 solution forms a sustained-release *in situ* hypergel that enhances cell transfection and extends gene expression. Oncology Letters. 17(3): 3085-3096.

Shubhra Q.T.H., Tóth J., Gyenis J., and Feczkó T. 2014. Surface modification of HSA containing magnetic plga nanoparticles by poloxamer to decrease plasma protein adsorption. Colloids and Surfaces B. 122: 529-536.

Singh-Joy S.D. and McLain V.C. 2008. Safety assessment of poloxamers 101, 105, 108, 122, 123, 124, 181, 182, 183, 184, 185, 188, 212, 215, 217, 231, 234, 235, 237, 238, 282, 284, 288, 331, 333, 334, 335, 338, 401, 402, 403, and 407, poloxamer 105 benzoate, and poloxamer 182 dibenzoate as used in cosmetics. International Journal of Toxicology. 27 Supplement 2: 93-128.

Song W., Zhang Y., Yu D.-G., Tran C.H., Wang M., Varyambath A., Kim J., and Kim I. 2021. Efficient synthesis of folate-conjugated hollow polymeric capsules for accurate drug delivery to cancer cells. Biomacromolecules. 22(2): 732-742.

Spiegel M., Kapusta K., Kołodziejczyk W., Saloni J., Żbikowska B., Hill G.A., and Sroka Z. 2020. Antioxidant activity of selected phenolic acids-ferric reducing antioxidant power assay and qsar analysis of the structural features. Molecules. 25(13): 3088.

Stenberg K., Skog S., and Tribukait B. 1985. Concentration-dependent effects of foscarnet on the cell cycle. Antimicrobial Agents and Chemotherapy. 28(6): 802-806.

Velma V., Dasari S.R., and Tchounwou P.B. 2016. Low doses of cisplatin induce gene alterations, cell cycle arrest, and apoptosis in human promyelocytic leukemia cells. Biomarker Insights 11: 113-121.

Vigani B., Faccendini A., Rossi S., Sandri G., Bonferoni M.C., Grisoli P., and Ferrari F. 2019. Development of a mucoadhesive *in situ* gelling formulation for the delivery of *Lactobacillus gasseri* into vaginal cavity. Pharmaceutics. 11(10): 511.

Vo T.N., Nguyen P.L., Tuong L.T., Vo P.N., Nguyen K.P.P., Nguyen N.S. 2012. Constituents of the leaves of pseuderanthemum carruthersii (seem.) Guill. var. atropurpureum (Bull.) Fosb. Phytochemistry Letters. 5(3):673-676.

Wahba H.M., AbouZid S.F., Sleem A.A., Apers S., Pieters L., Shahat A.A. 2011. Chemical and biological investigation of some *clerodendrum* species cultivated in Egypt. Pharmaceutical Biology. 49(1): 66-72.

Warinthip, N., Liawruangrath, B., Natakankitkul, S., Rannurags, N., Pyne, S.G., and Liawruangrath, S. 2023. Chemical constituents antioxidant and antibacterial activities of the leaves and flowers from *Gardenia carinata* Wallich. Natural and Life Sciences Communications. 22(1): e2022004.

Wong K. and Tan C. 2005. Volatile constituents of the flowers of *Clerodendron fragrans* (vent.) r. Br. Flavour and Fragrance Journal. 20: 429-430.

Zhang H. and Tsao R. 2016. Dietary polyphenols, oxidative stress and antioxidant and anti-inflammatory effects. Current Opinion in Food Science. 8: 33-42.

Zhang Y., Song W., Lu Y., Xu Y., Wang C., Yu D.-G., and Kim I. 2022. Recent advances in poly (α-l-glutamic acid)-based nanomaterials for drug delivery. Biomolecules. 12(5): 636.

Zhang Y., Yuan Y., Wu H., Xie Z., Wu Y., Song X., Wang J., Shu W., Xu J., Liu B. et al. 2018. Effect of verbascoside on apoptosis and metastasis in human oral squamous cell carcinoma. International Journal of Cancer. 143(4): 980-991.

Zulfiayu S., Paulus P., Arlan K.I., Prisca Safriani W., and Rizka Puji Astuti D. 2020. Determination of total flavonoid levels of ethanol extract sesewanua leaf (*Clerodendrum fragrans* wild) with maceration method using UV-Vis spectrofotometry. Pharmacognosy Journal. 12(2): 356-360.

OPEN access freely available online
Natural and Life Sciences Communications
Chiang Mai University, Thailand. https://cmuj.cmu.ac.th